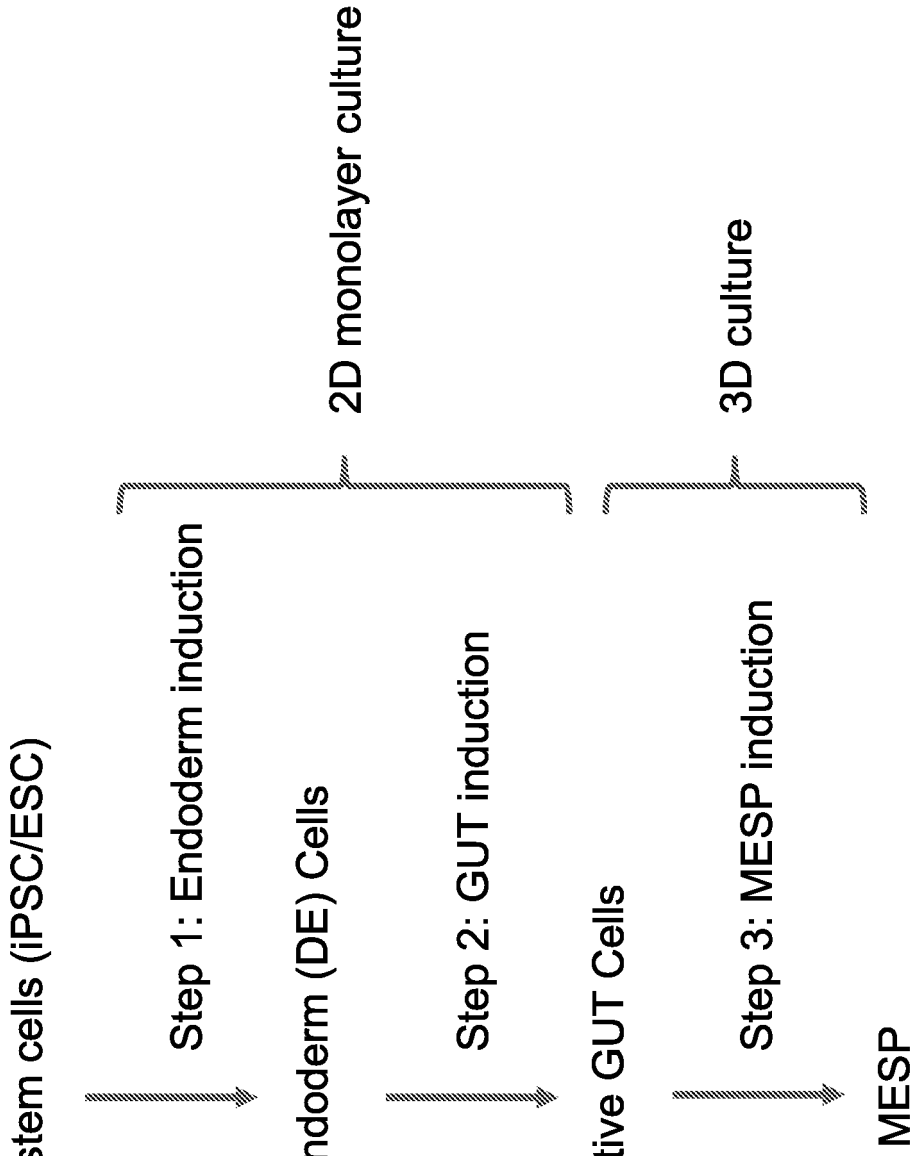


Fig. 1. Schematic of MESP derivation from pluripotent stem cells.

Fig. 2. Induction of Definitive Endoderm (DE) and GUT markers during differentiation of PSC to MESP

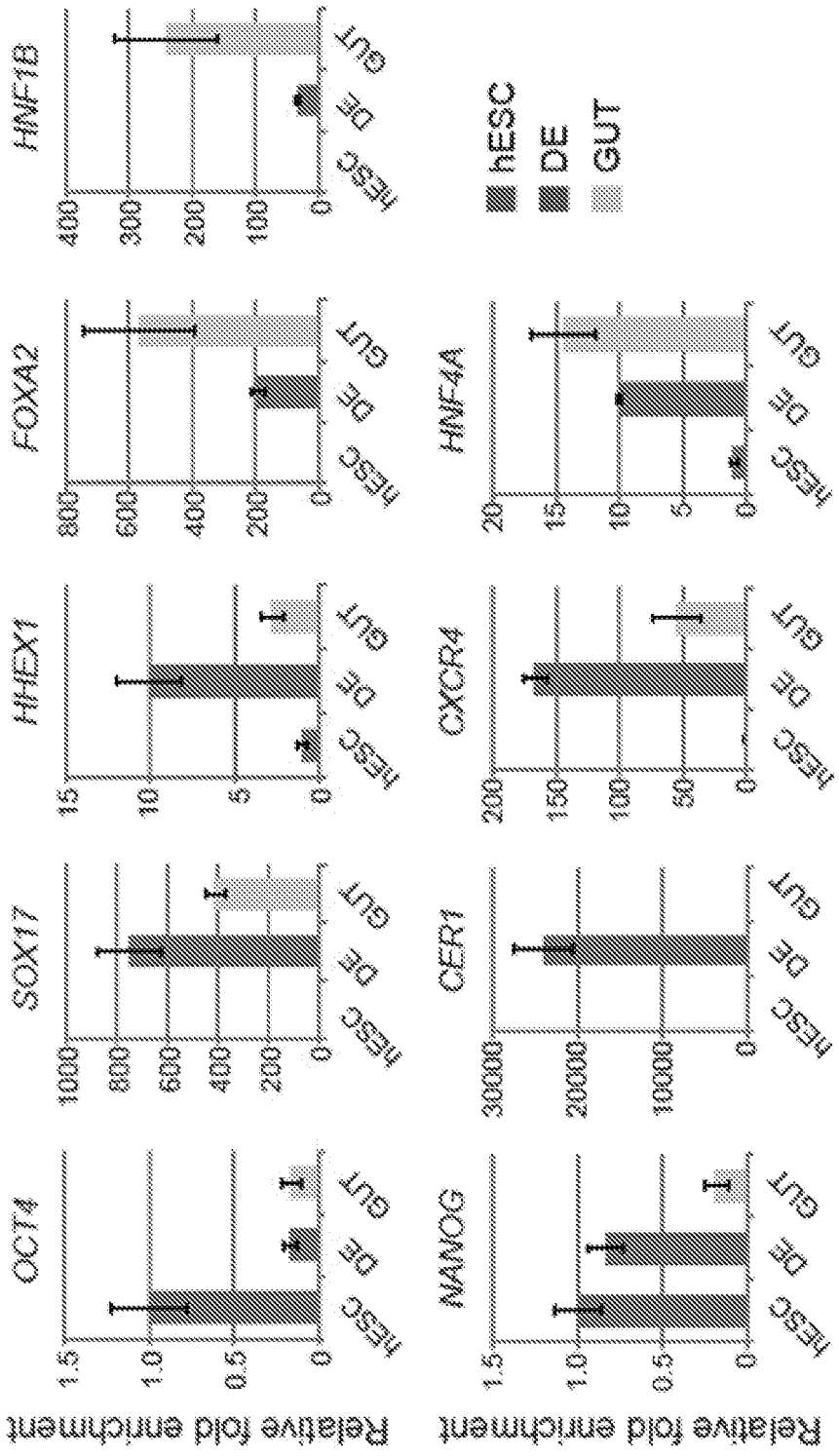


Fig. 3A

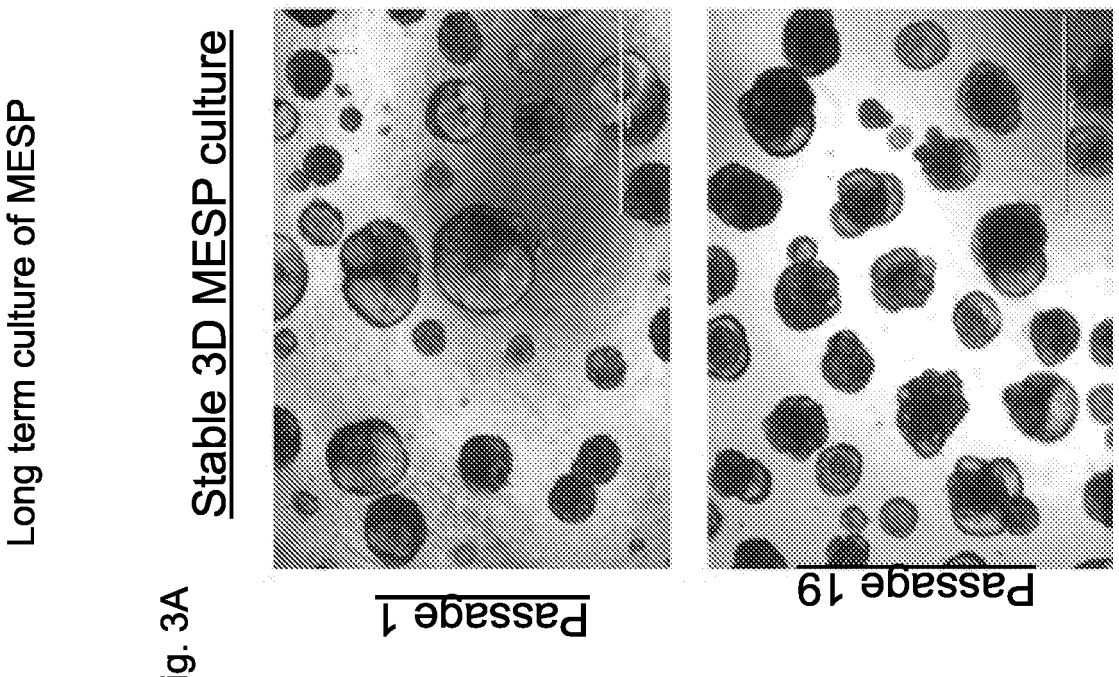

Long term culture of MESP
Stable 3D MESP culture
Passage 1
Passage 19

Fig. 3B

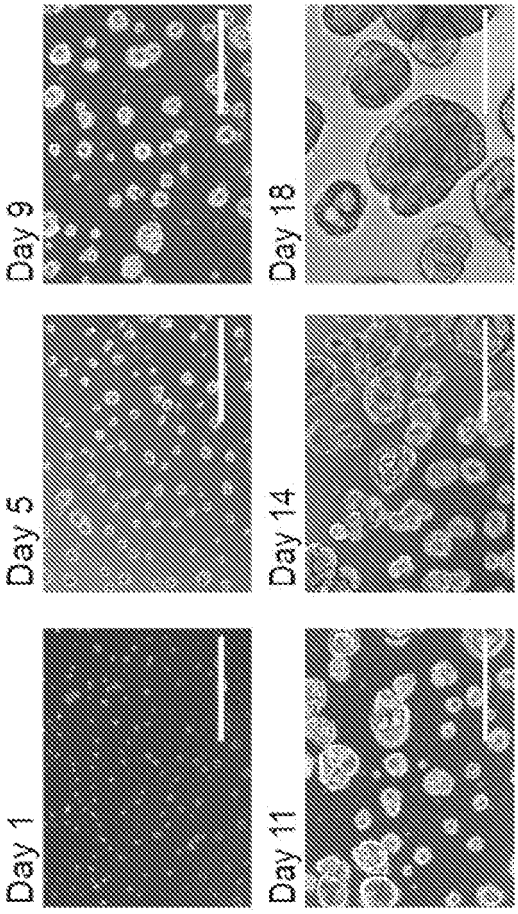

Day 1
Day 5
Day 9
Day 11
Day 14
Day 18

Fig. 4. MESP expresses markers of the posterior Foregut

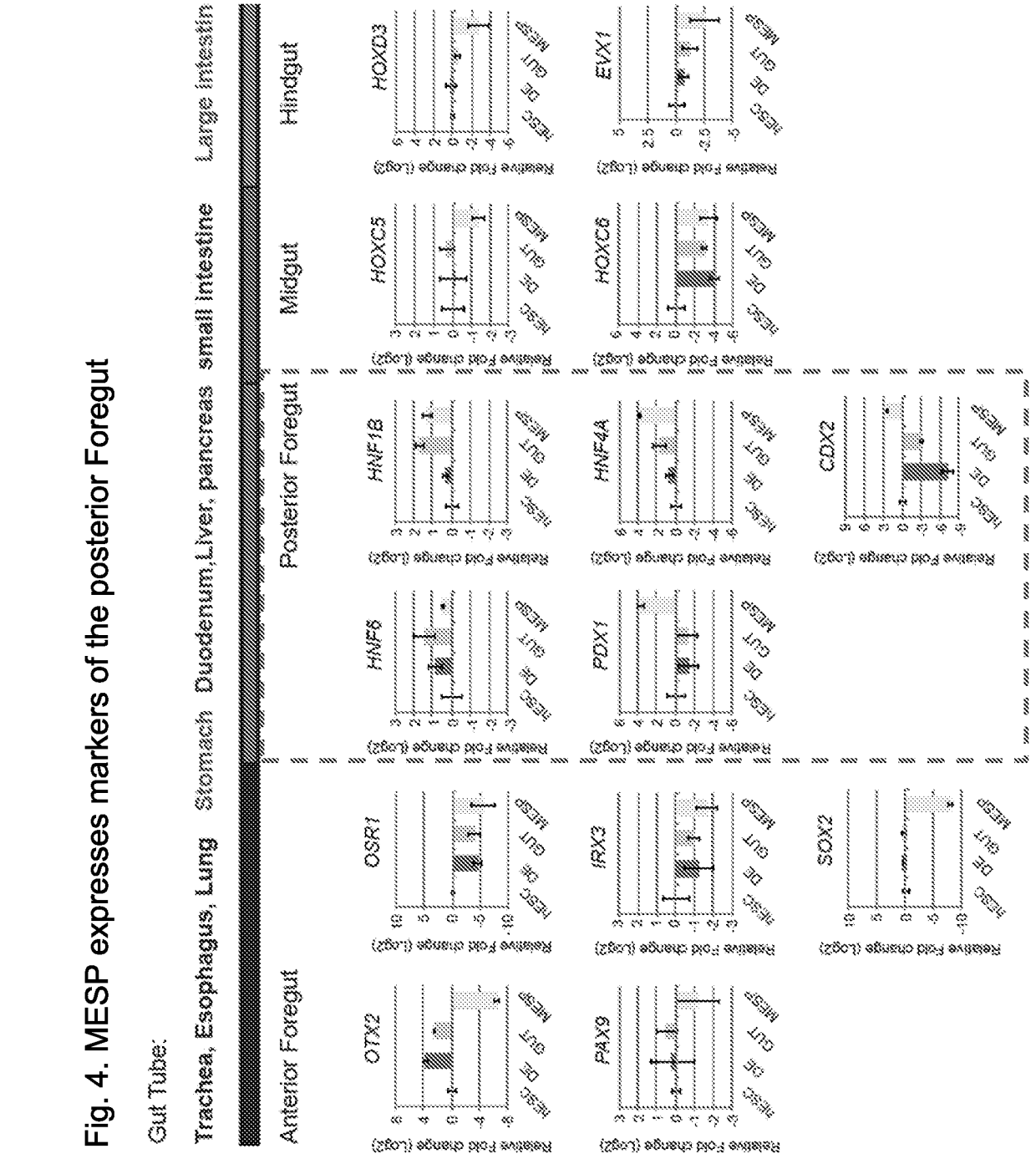


Fig. 5A

Homogenous Expression of stem cell markers in MESP

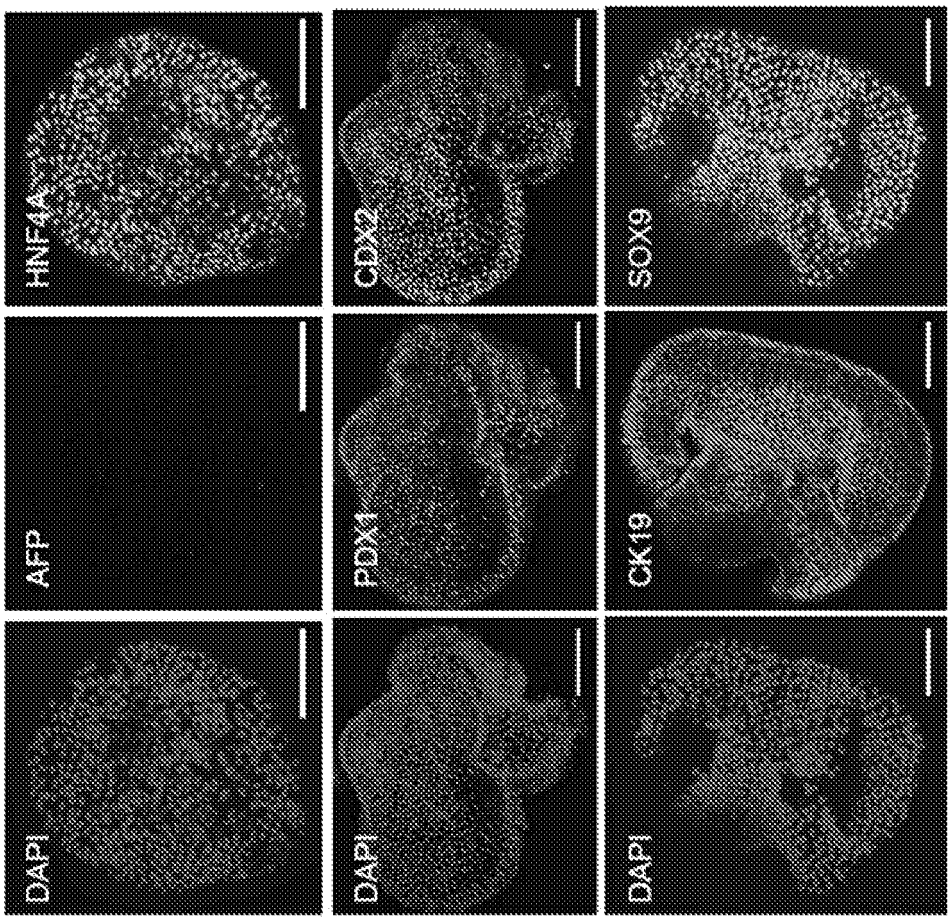
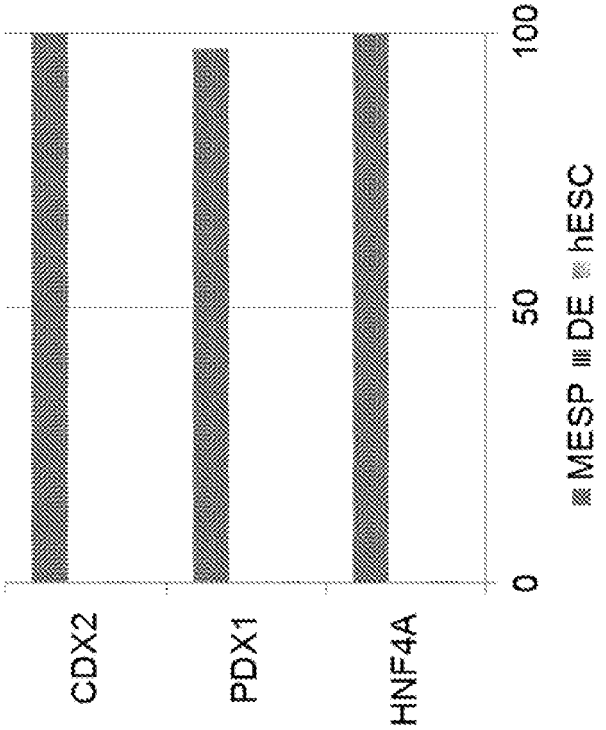


Fig. 5B



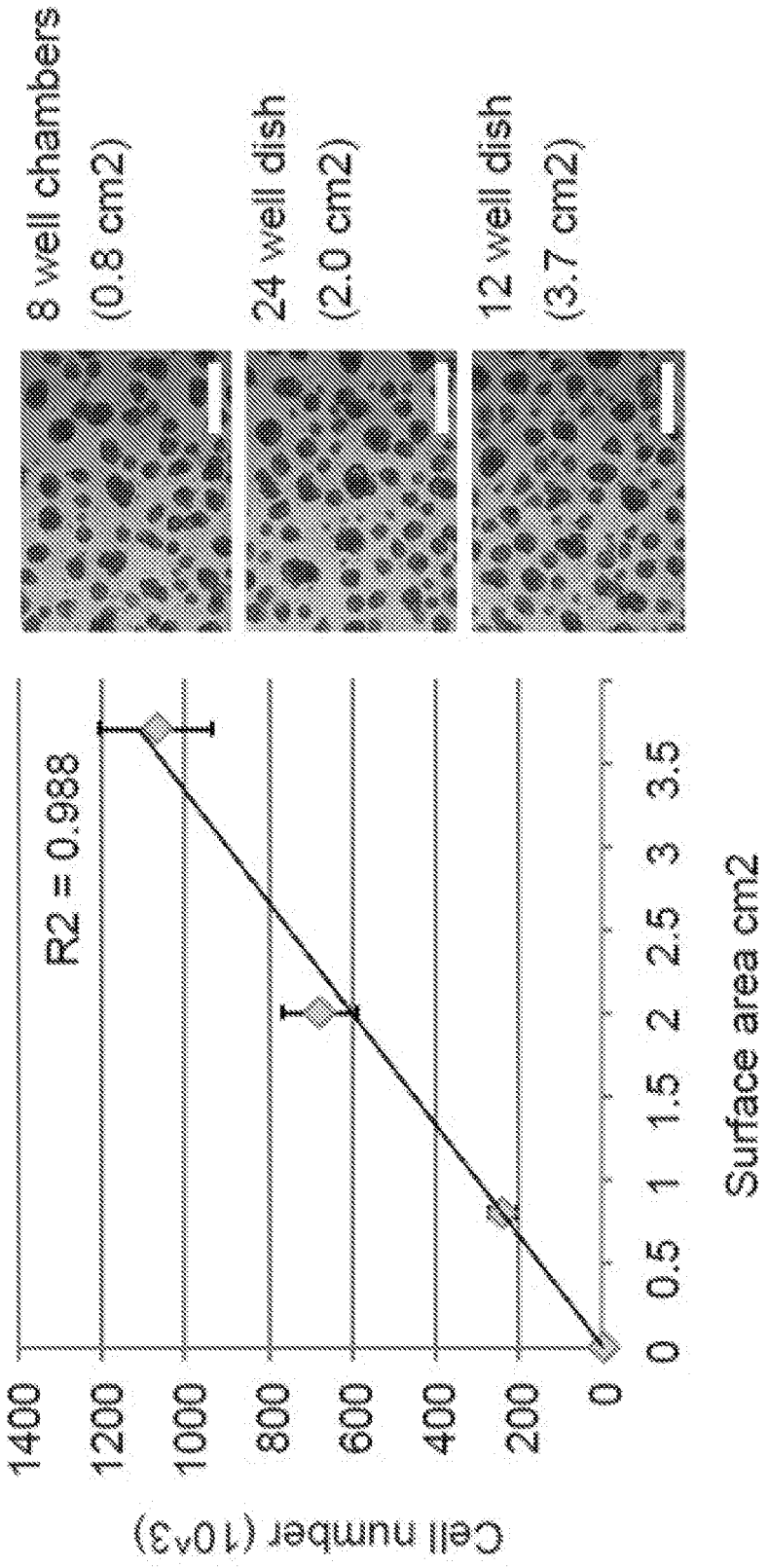


Fig. 6. Scalability of MESP culture system

Fig. 7A

Stable long term MESP culture

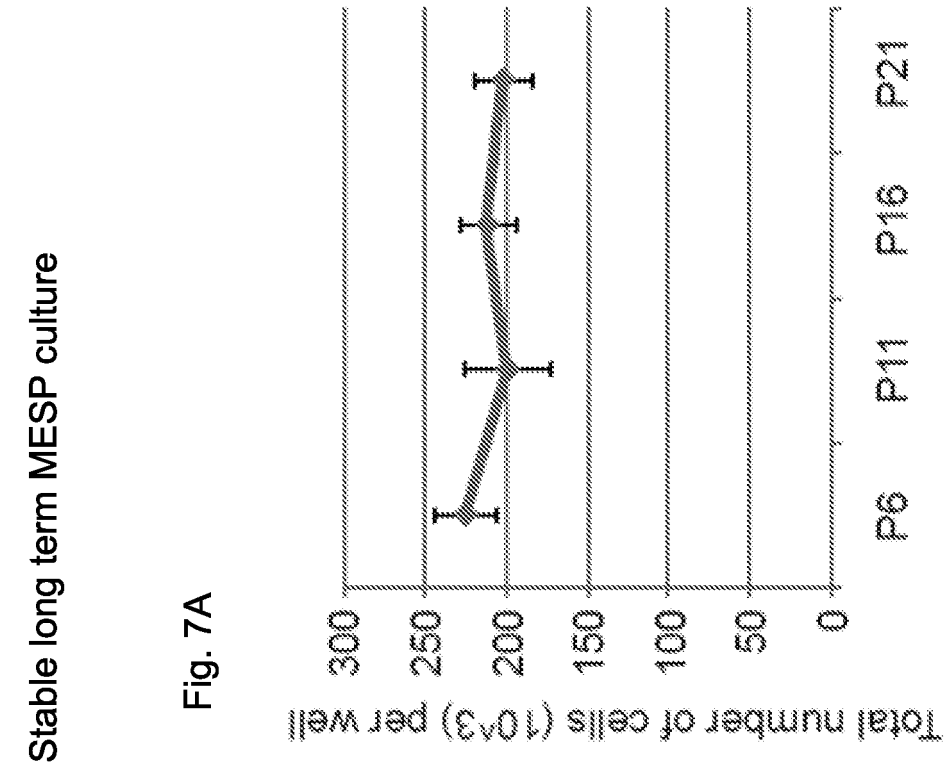
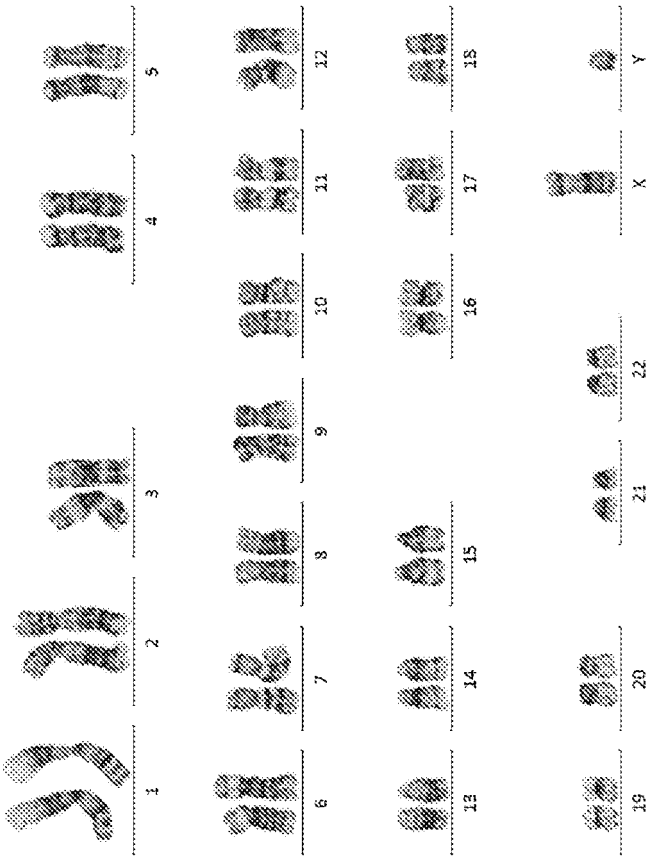


Fig. 7B



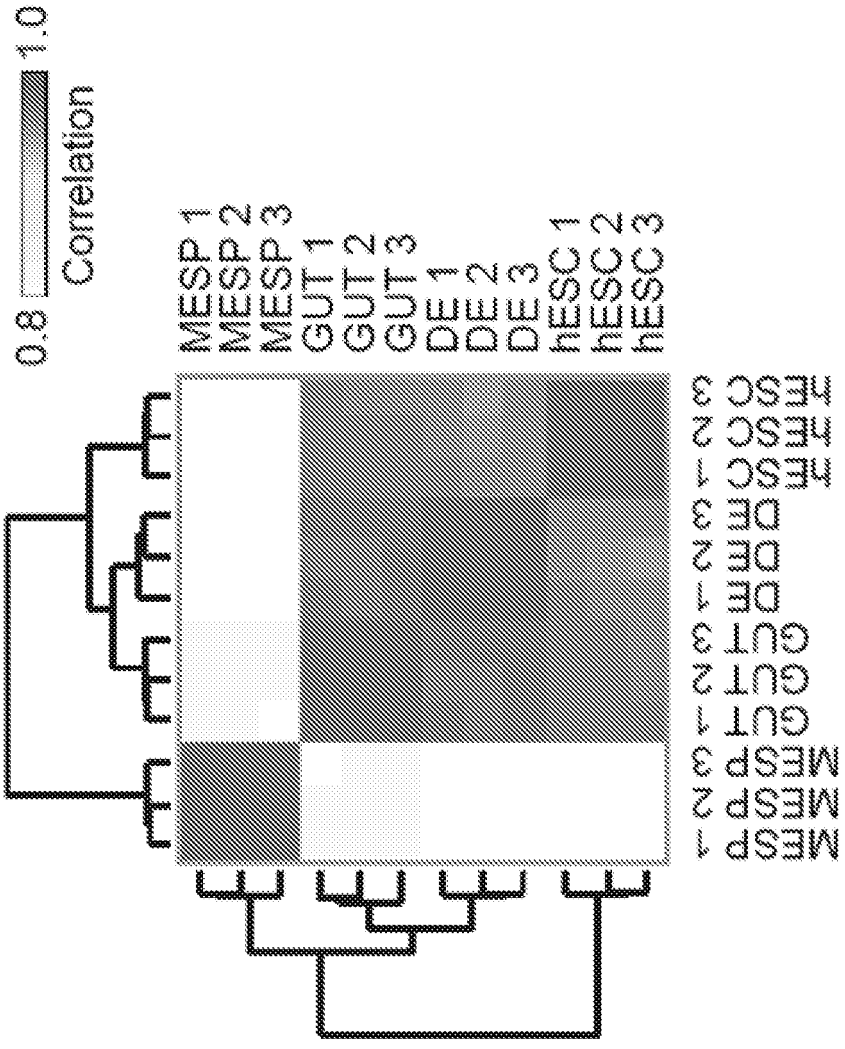


Fig. 8: Transcriptome of MESP is different from hESC, DE and GUT

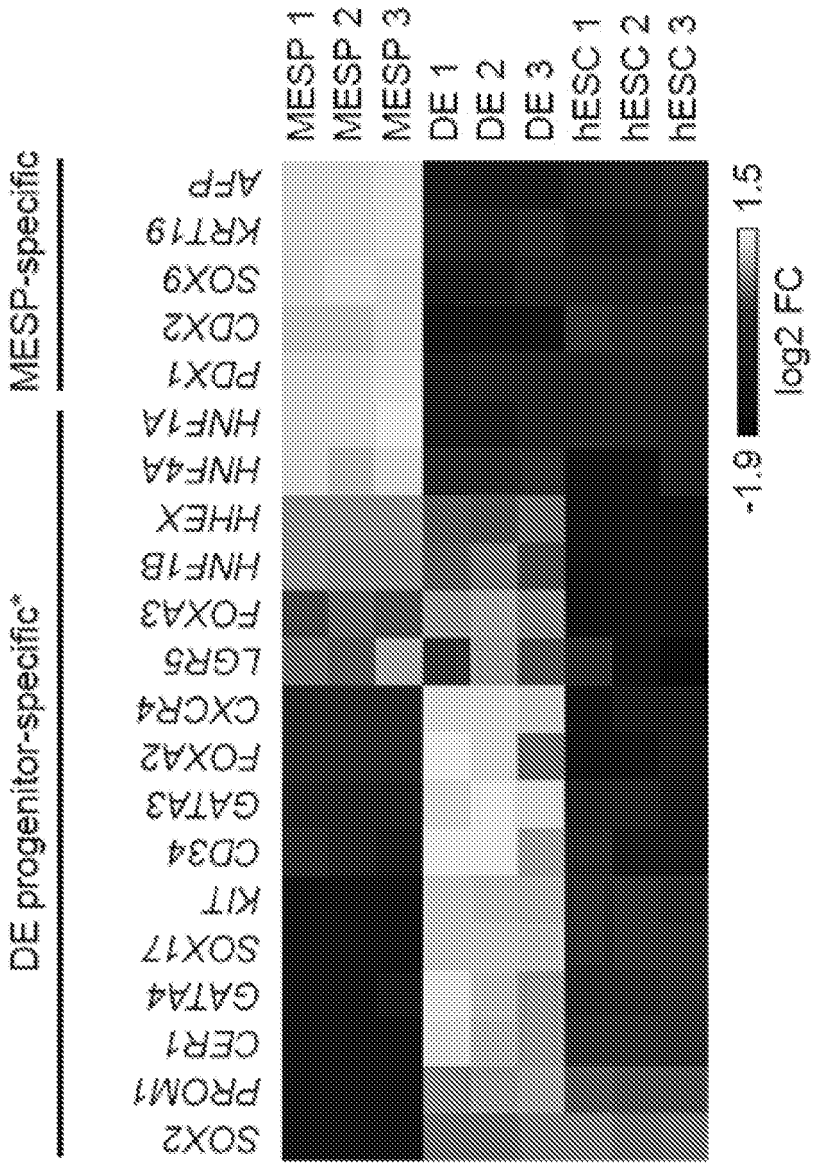


Fig. 9: MESP do not express DE progenitor-specific genes

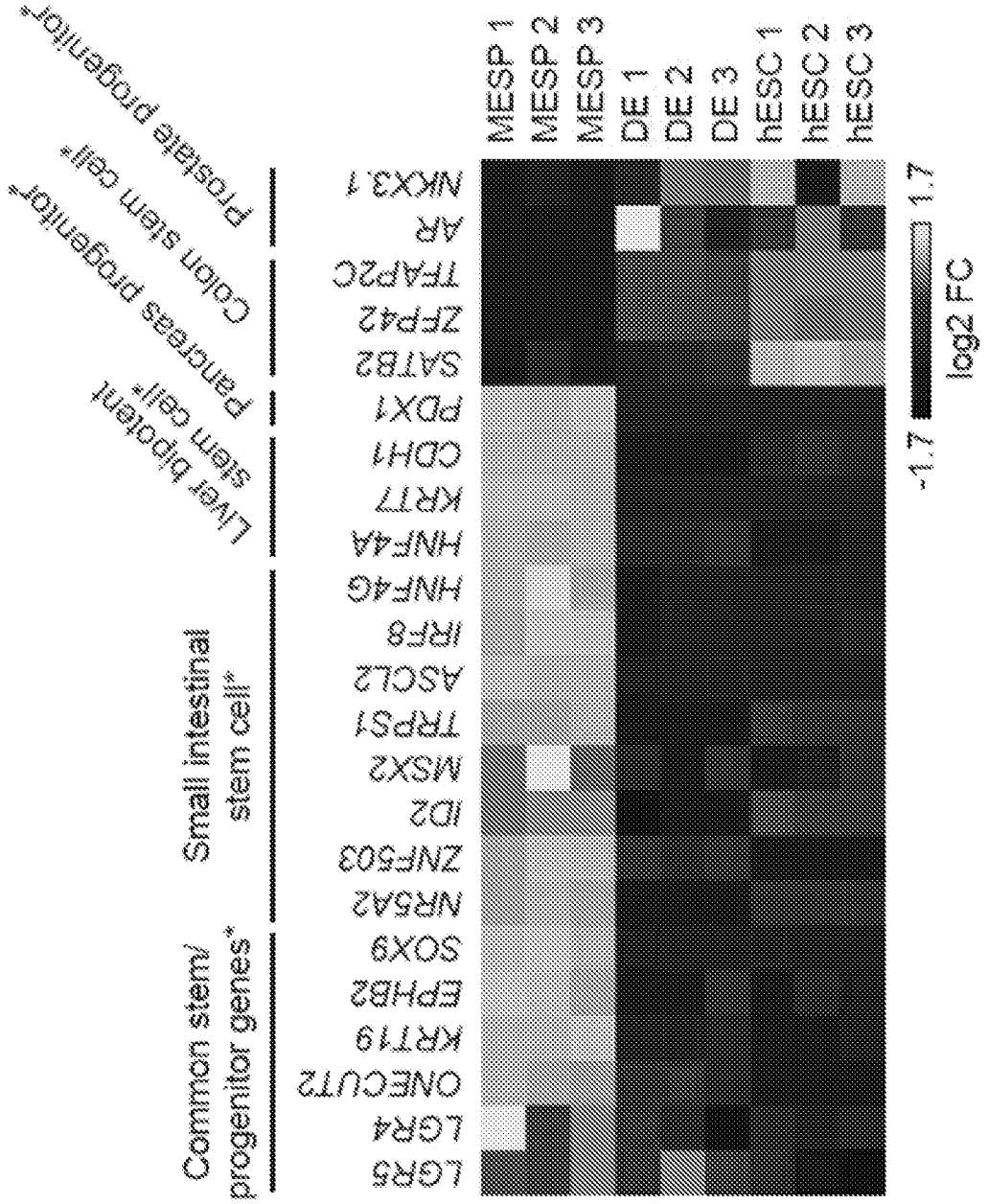


Fig. 10: MESP express many genes found in fetal and adult stem cells.

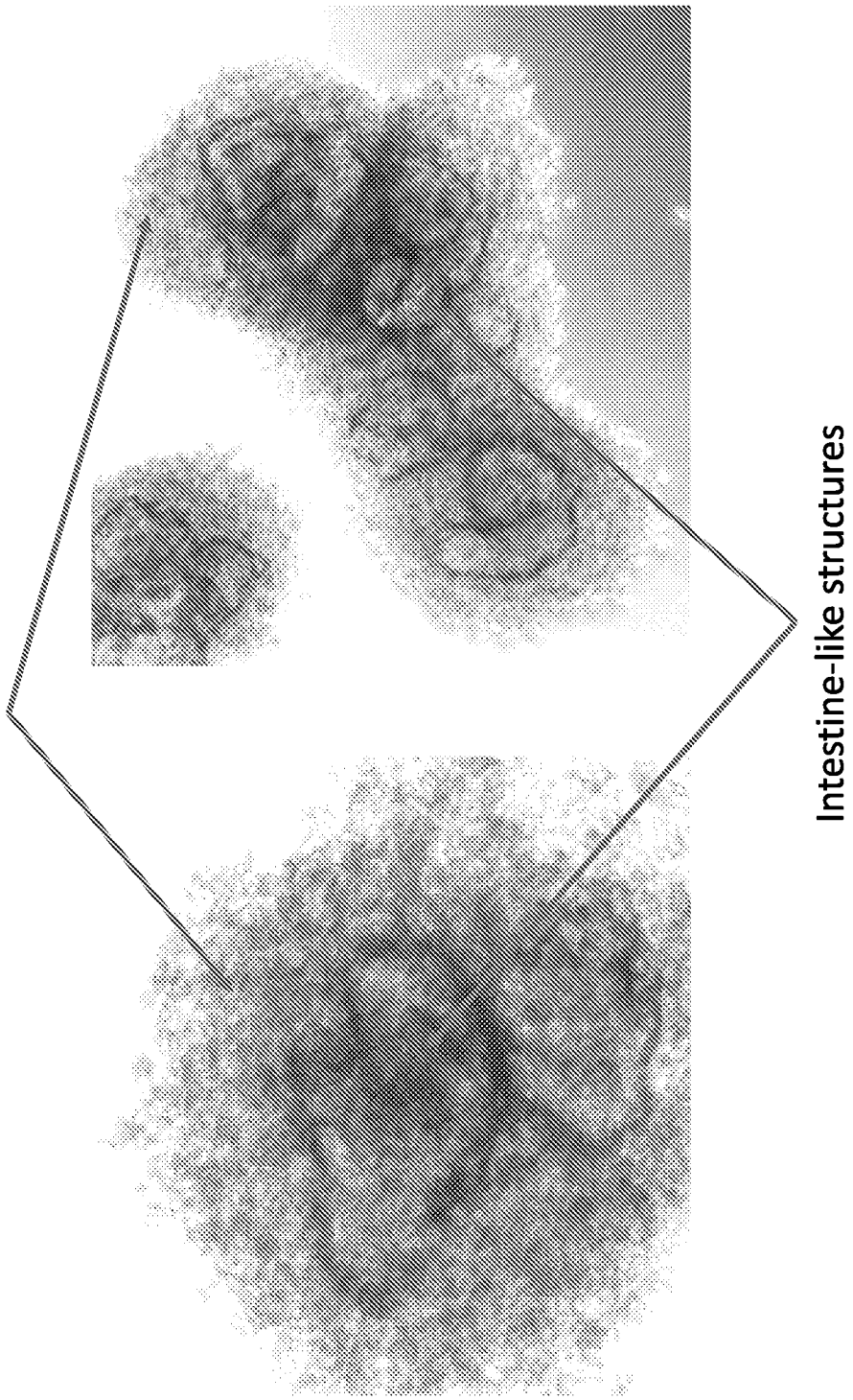


Fig. 11: Intestinal organoid generated from MESP

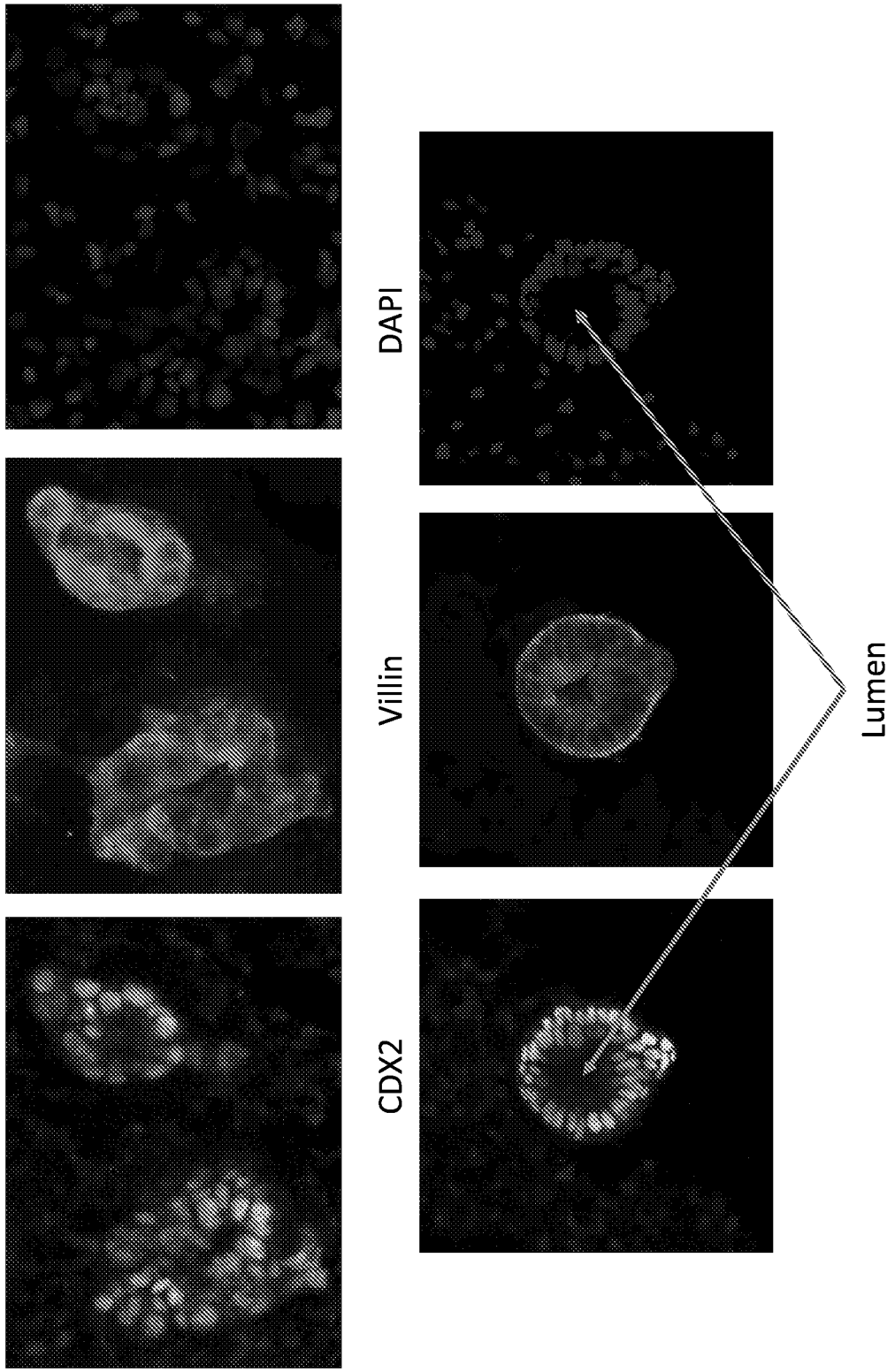


Fig.12: Intestinal organoid expresses intestinal tissue markers CDX2 and Villin.

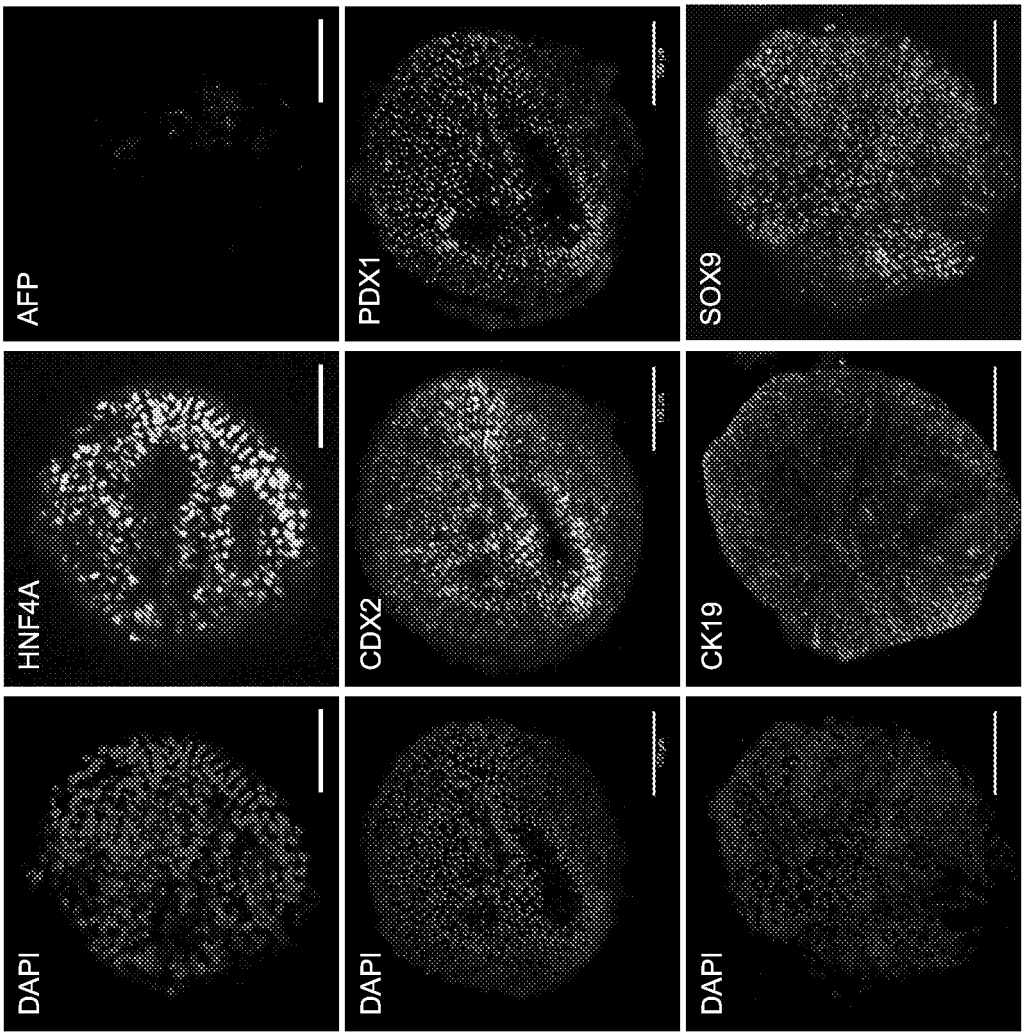


Fig.13: MESP can be generated from induced pluripotent stem cells (iPSC)

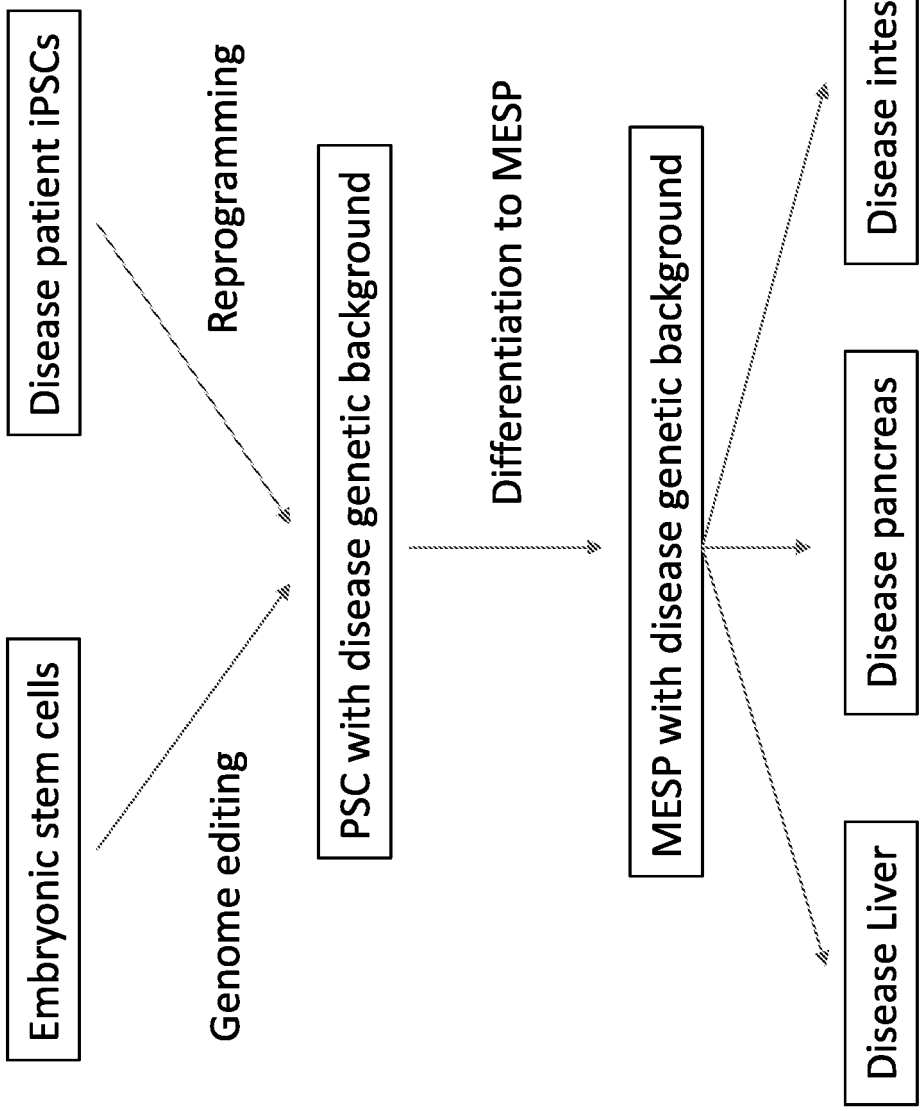
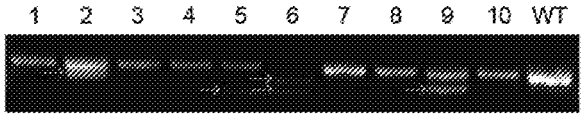


Fig. 14: Generating disease models of multiple organs with MESP

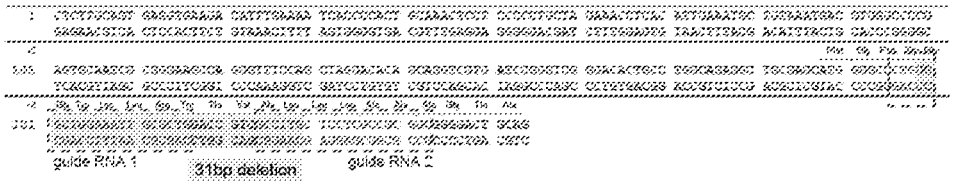
Modeling hypercholestrolemia with Low Density Lipoprotein Receptor (LDLR) knockout MESP

Fig. 15A

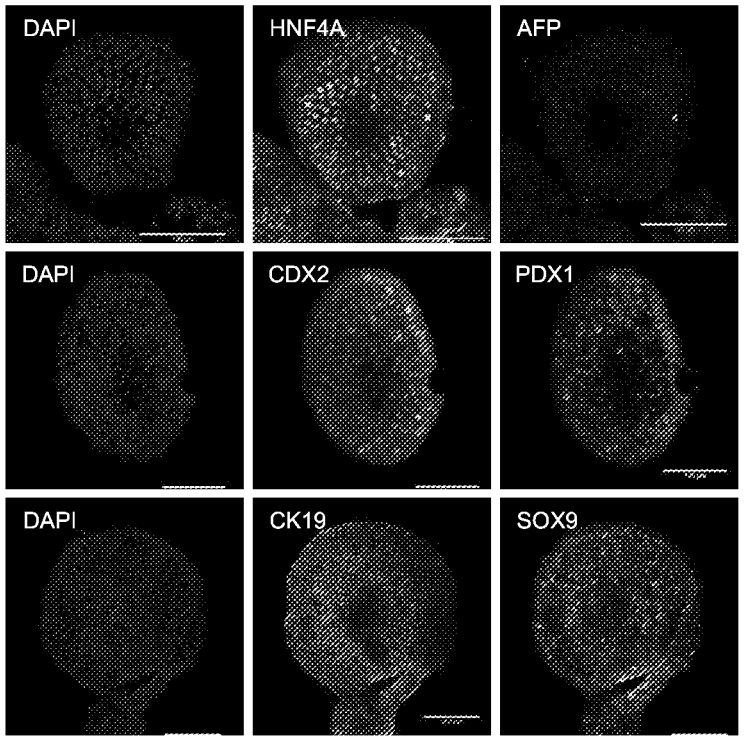


Type	Number	Percentage
Wild-type clones	40	83.3%
Heterozygous mutant clones	6	12.5%
Compound heterozygous mutant clones	2	4.2%
Total mutant clones	8	16.7%
Total clones picked	48	100%

Fig. 15B



C)



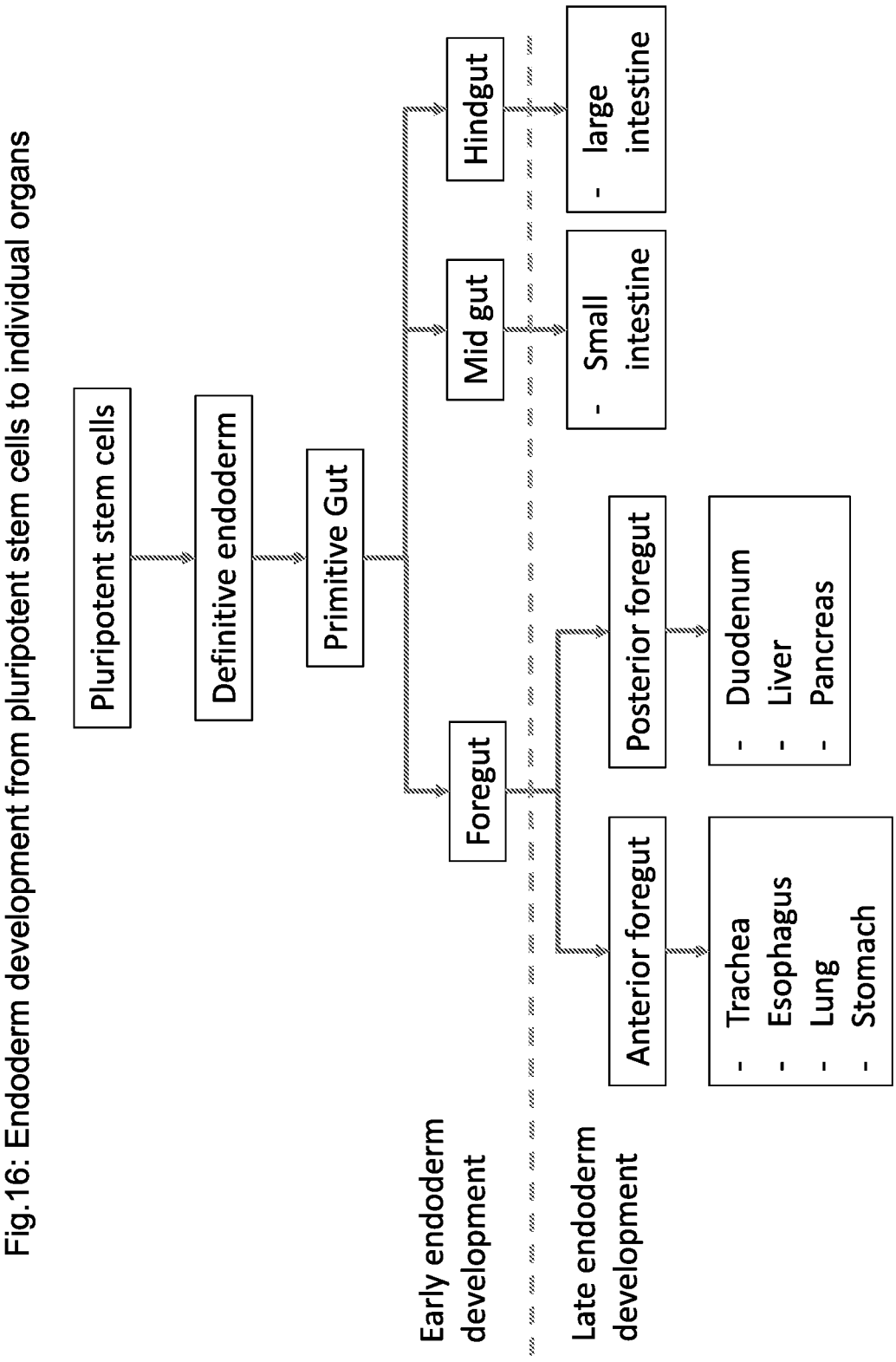


Fig.16: Endoderm development from pluripotent stem cells to individual organs

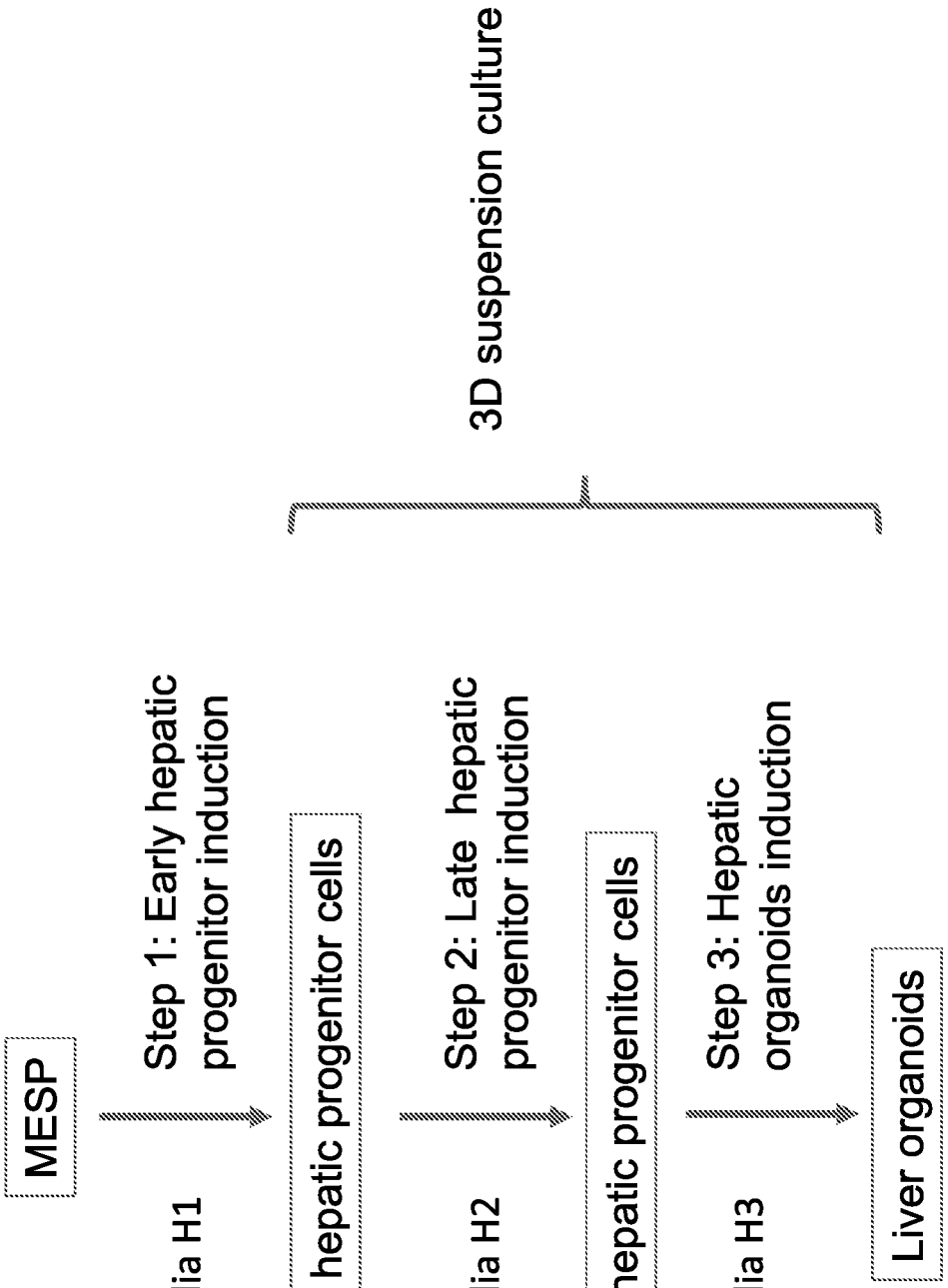
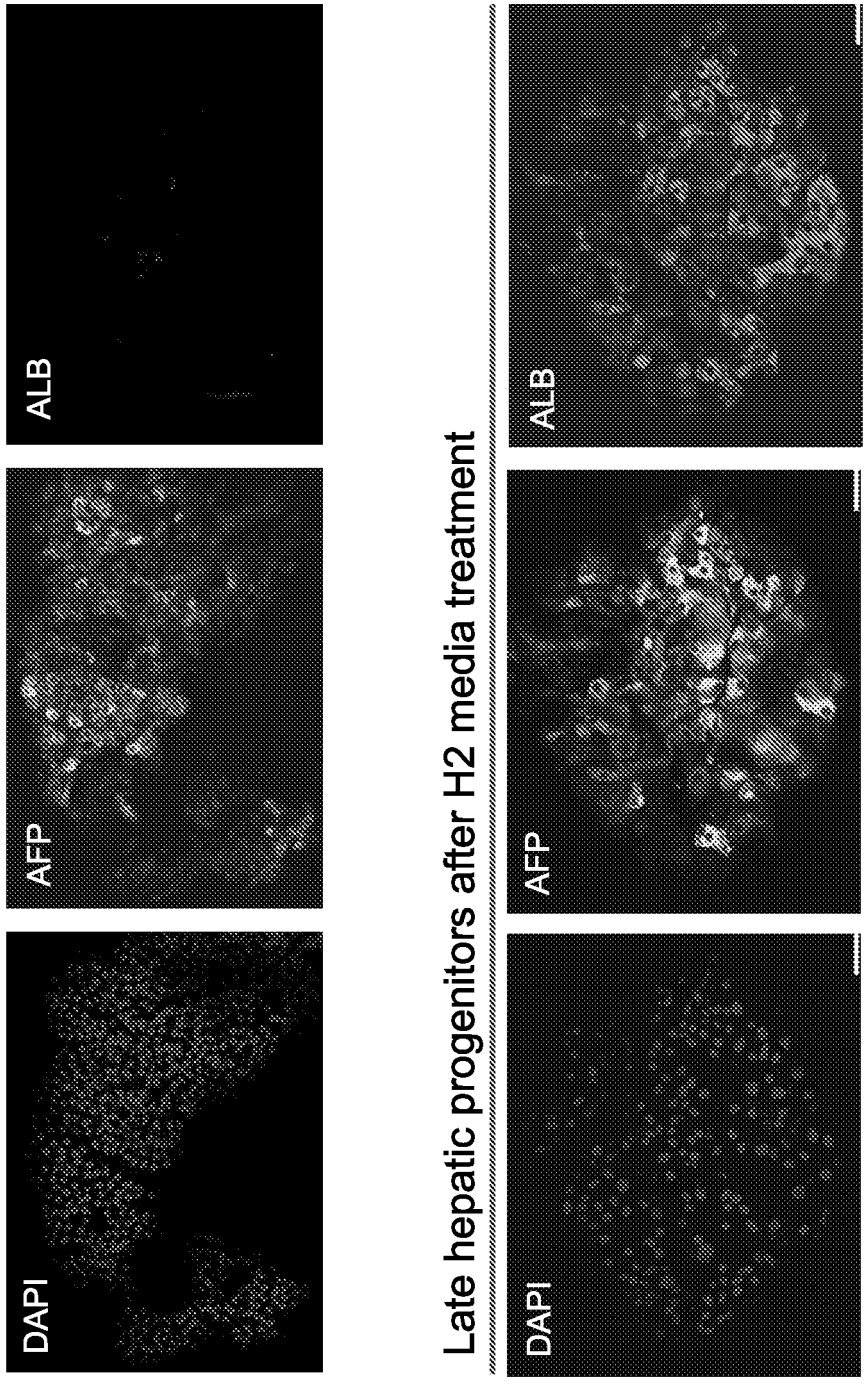


Fig. 17. Schematic of Liver organoid differentiation from MESP.

Fig. 18. Expression of hepatic markers in progenitors after H1 and H2 treatment



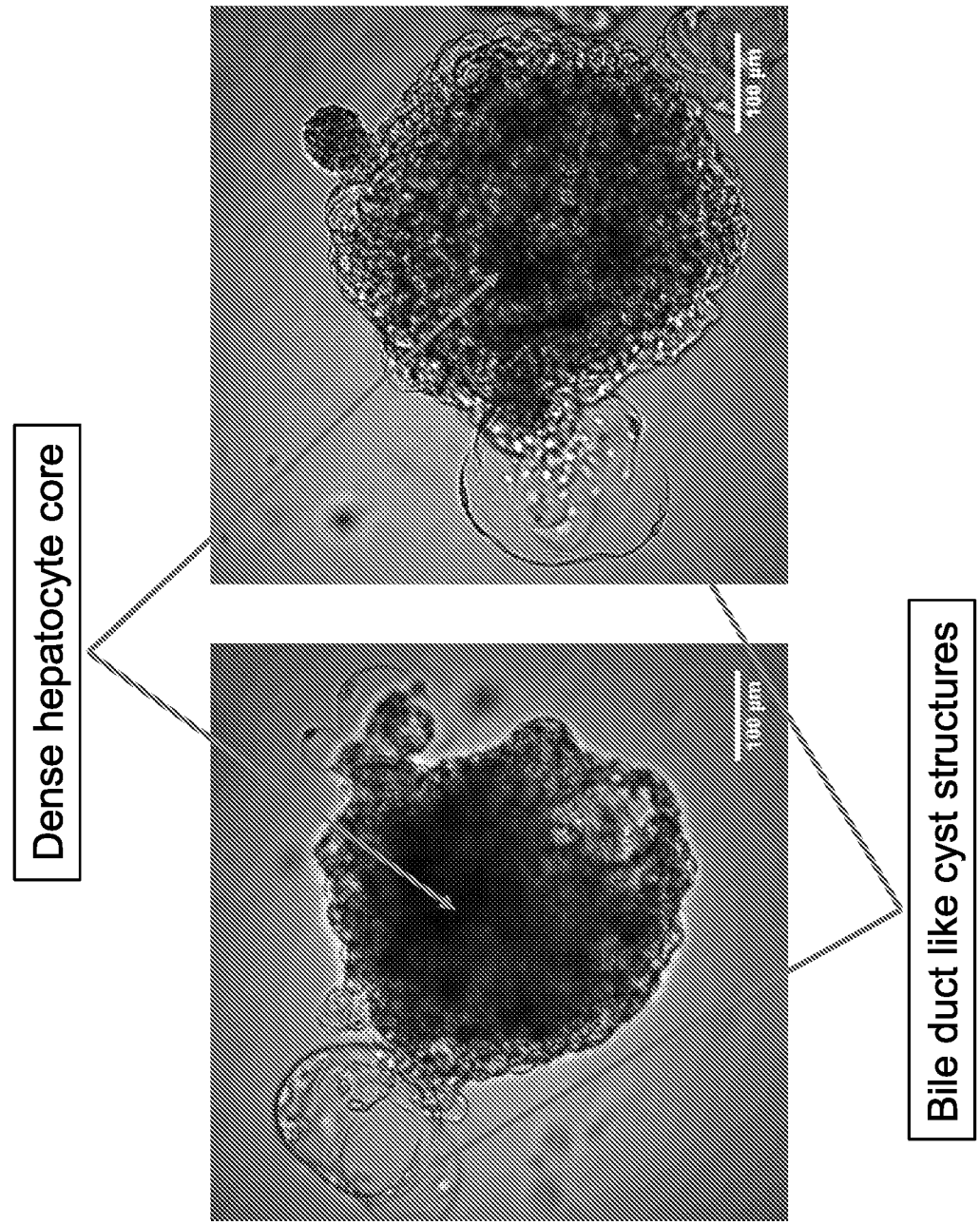


Fig. 19. Bright filed images of hepatic organoids differentiated from MESP.

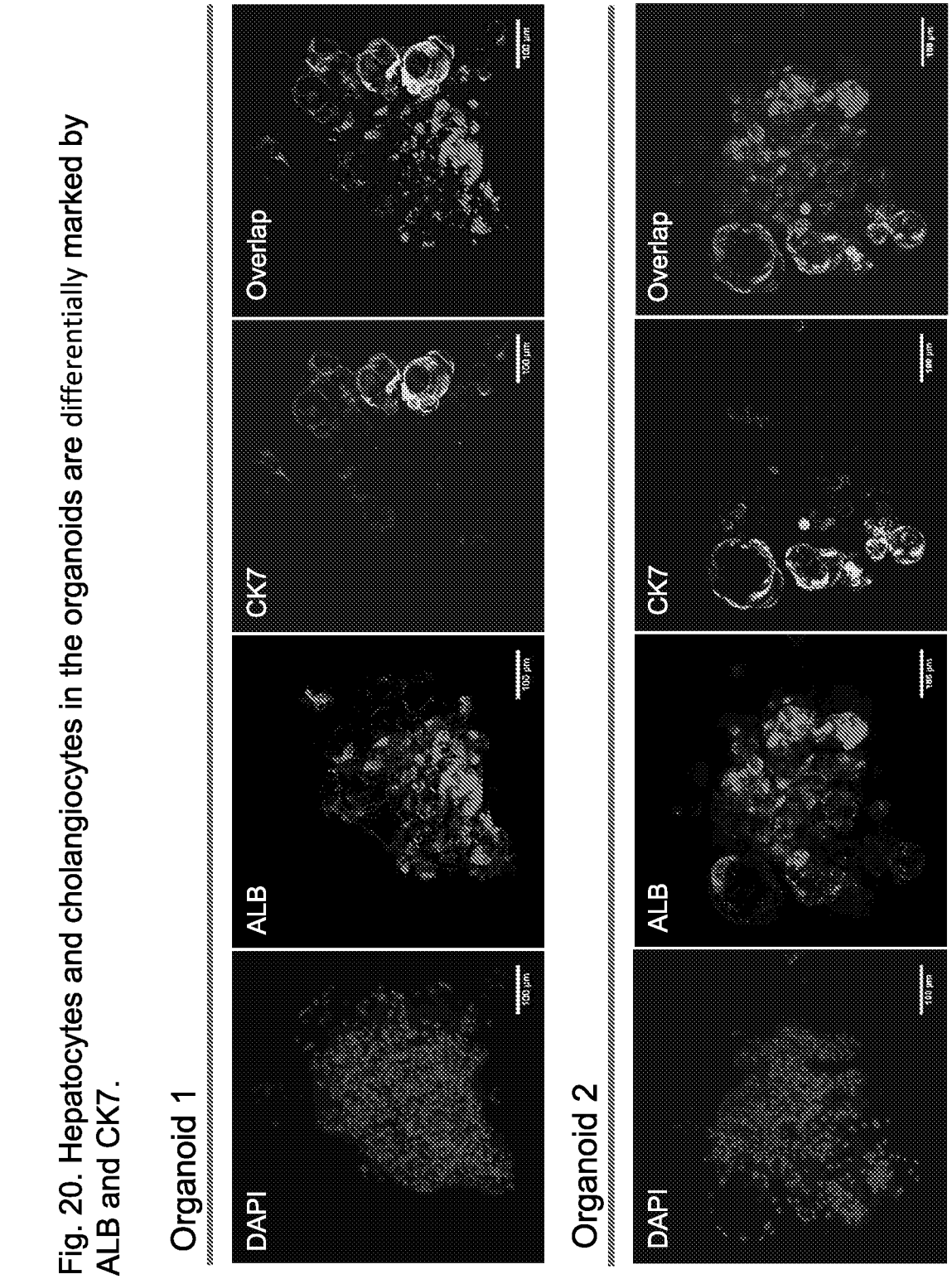


Fig. 20. Hepatocytes and cholangiocytes in the organoids are differentially marked by ALB and CK7.

Similar arrangement of hepatocytes and cholangiocytes in the organoids compared to the liver lobule

Fig. 21A

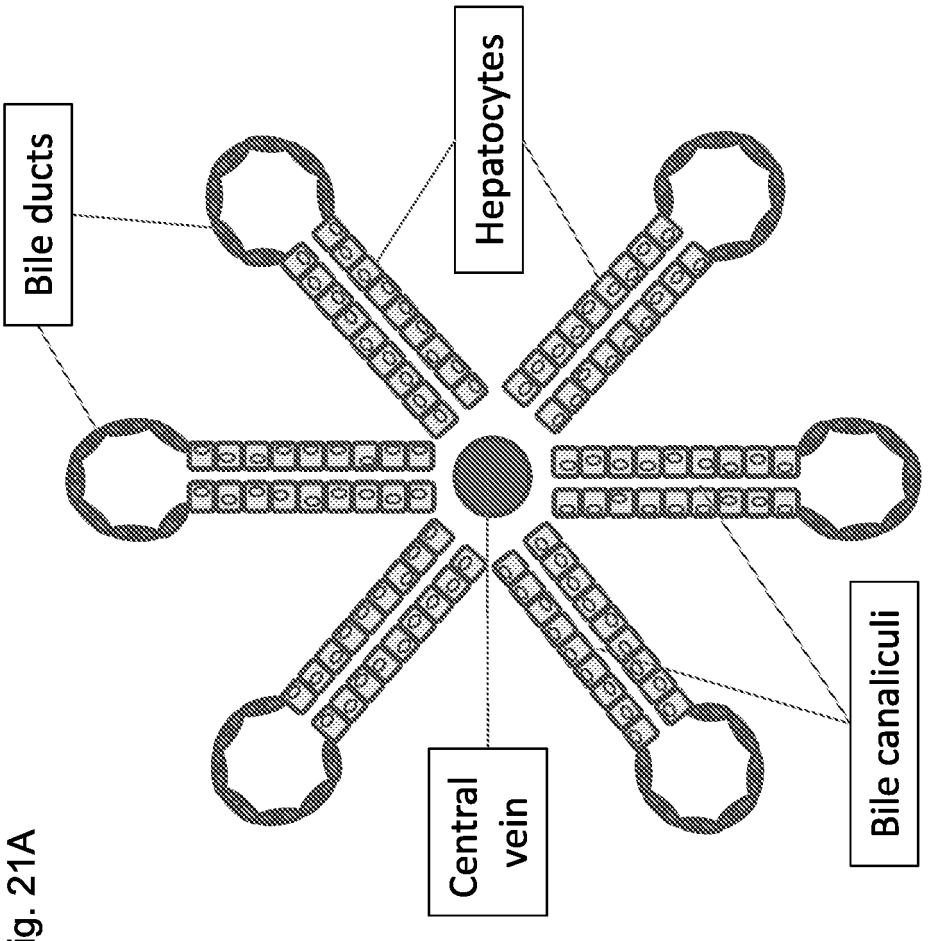
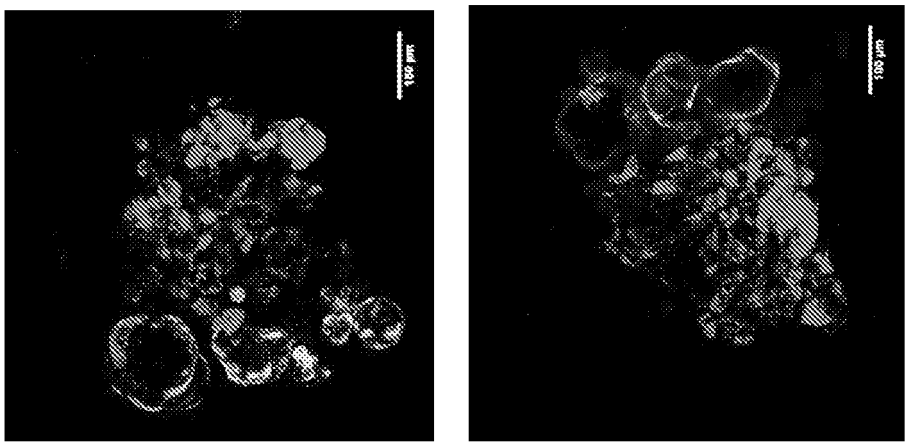


Fig. 21B



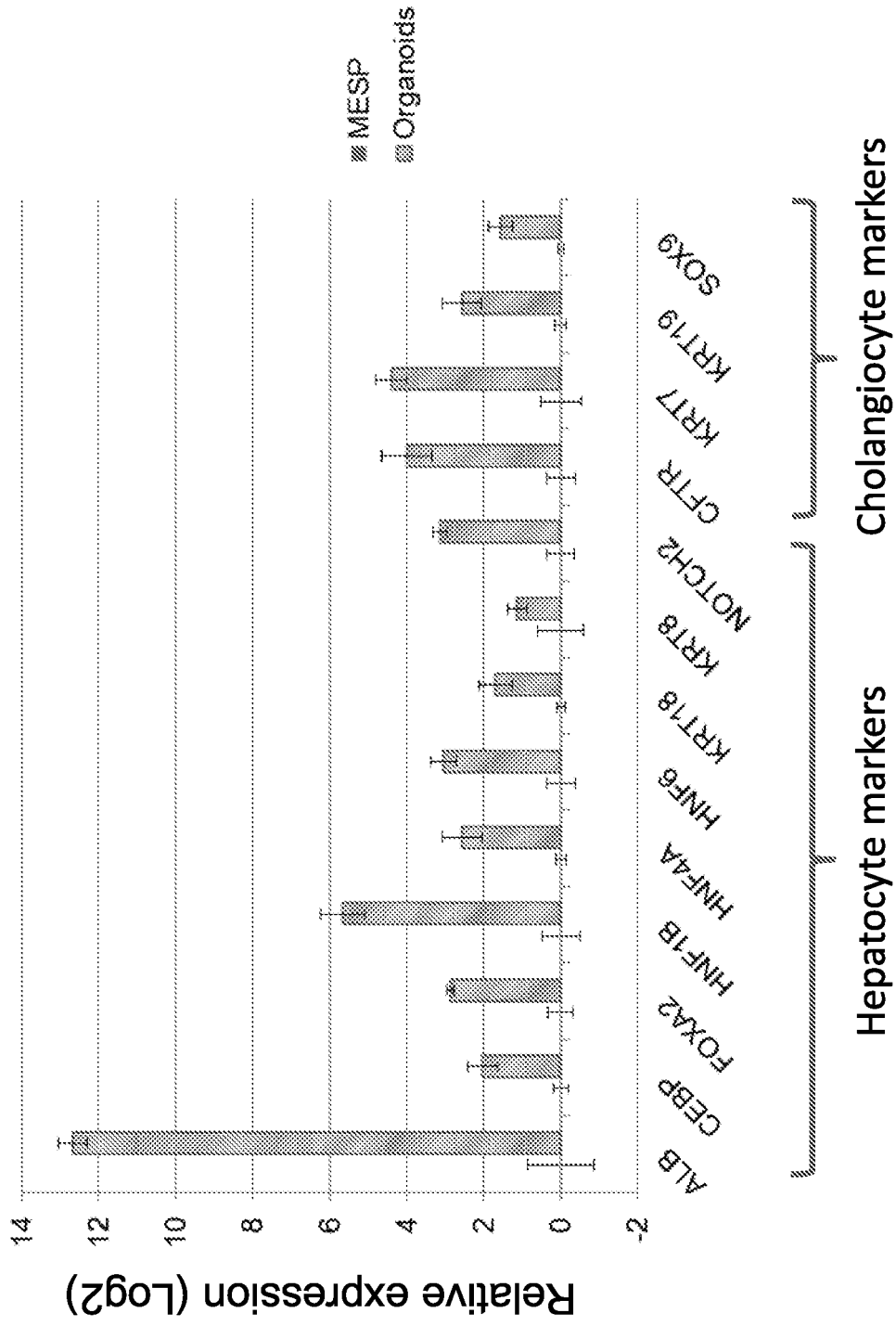


Fig. 22. Expression of liver tissue genes in the hepatic organoids.

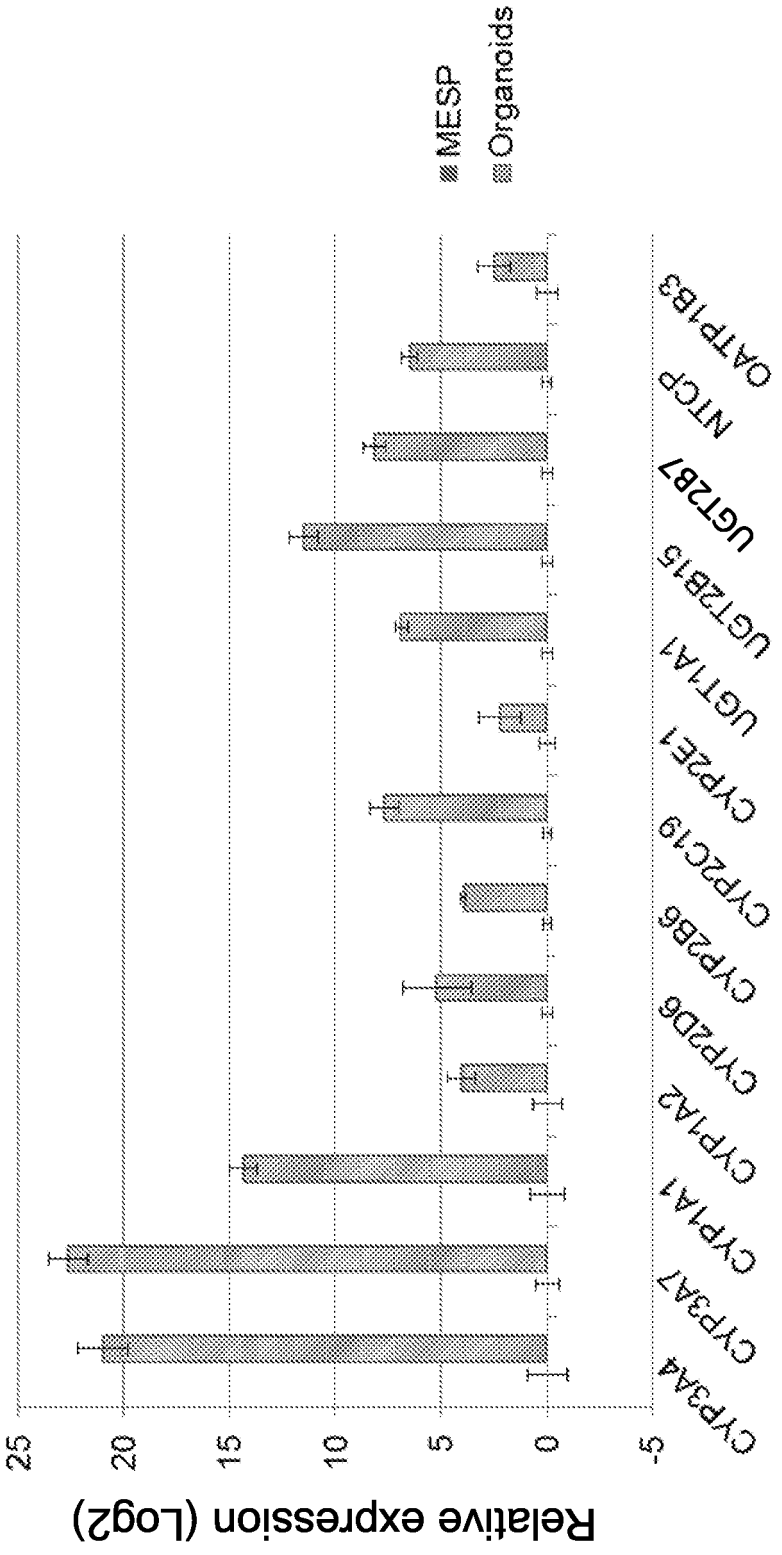


Fig. 23. Expression of liver specific enzymes and transporter in the hepatic organoids.

Expression of transporter MRP2 in liver organoids

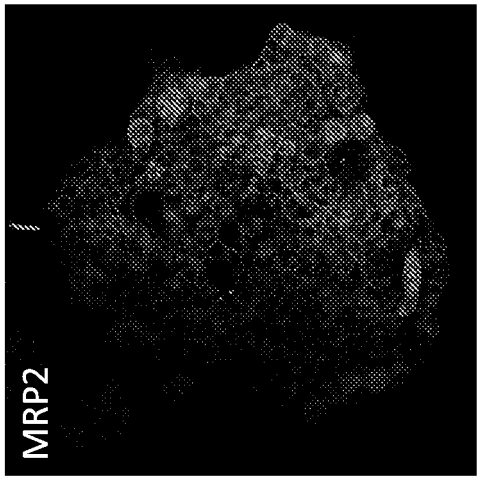


Fig. 24A

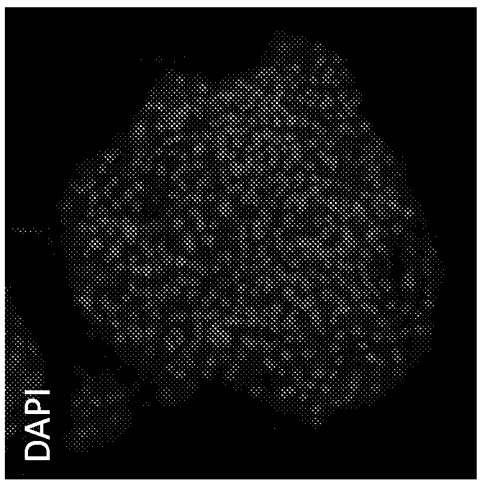
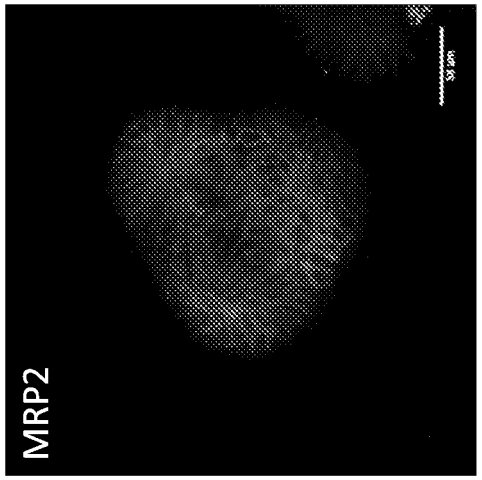
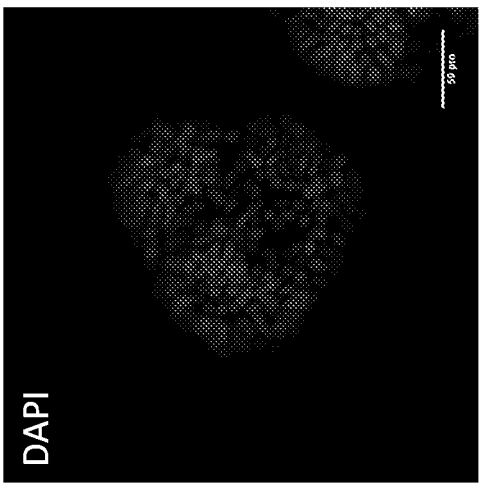


Fig. 24B





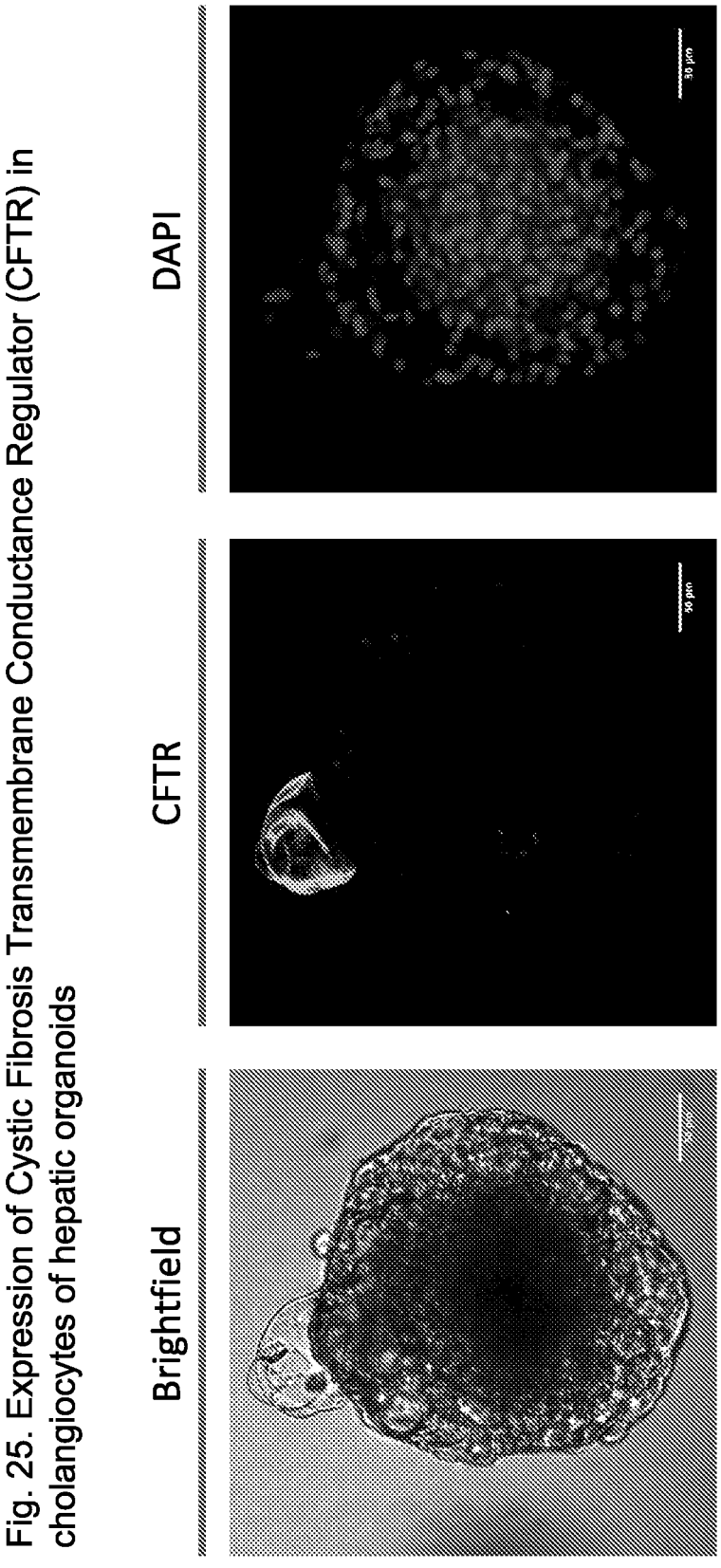


Fig. 25. Expression of Cystic Fibrosis Transmembrane Conductance Regulator (CFTR) in cholangiocytes of hepatic organoids

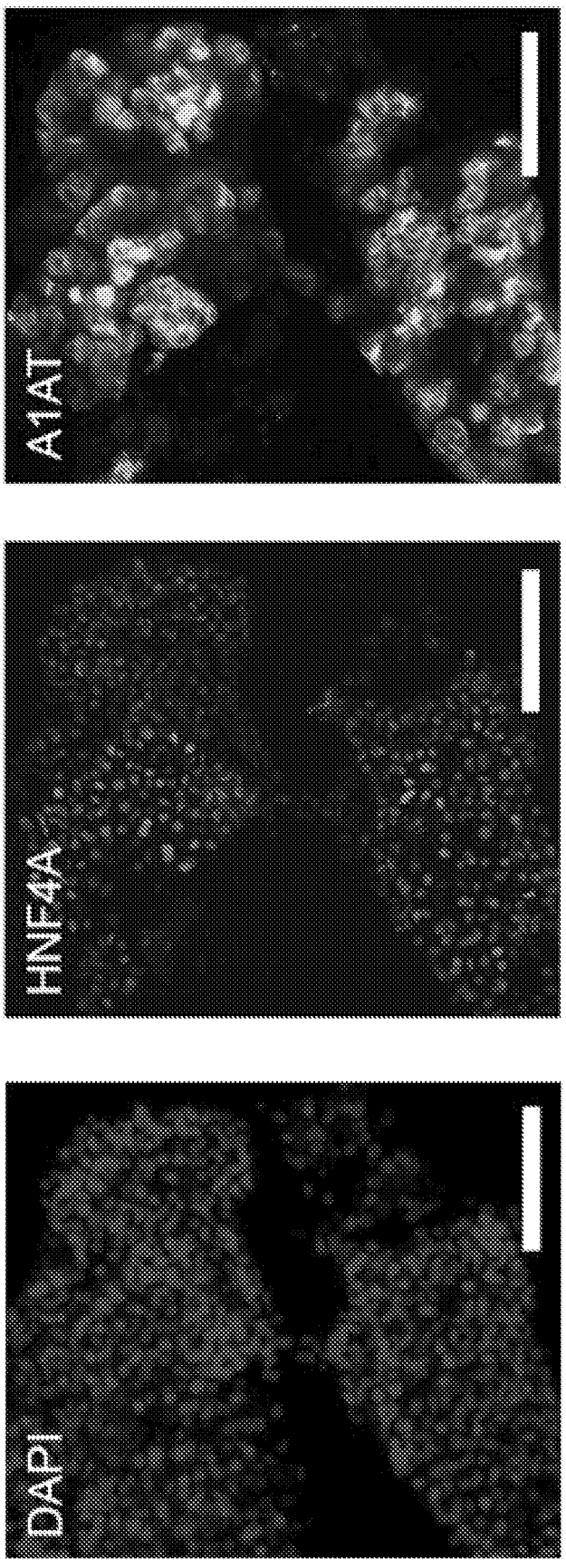


Fig. 26. Expression of liver specific marker Alpha-1 Antitrypsin (A1AT) .

Glycogen storage and lipid uptake by the hepatocytes in the hepatic organoid.

Fig. 27A PAS staining

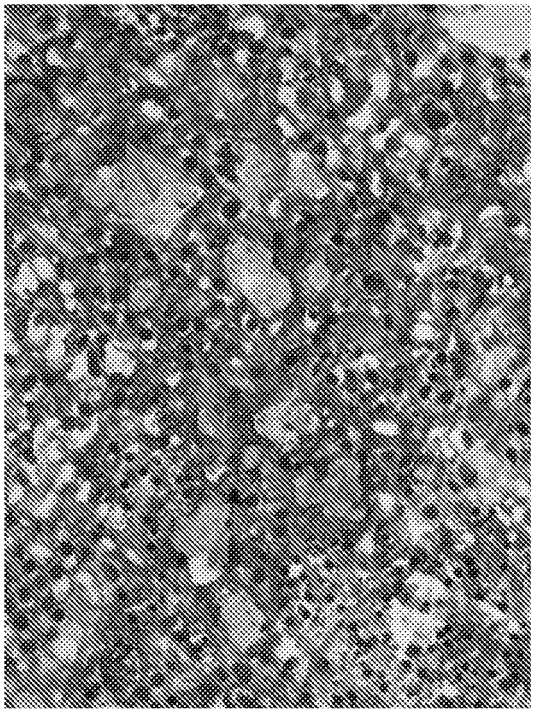
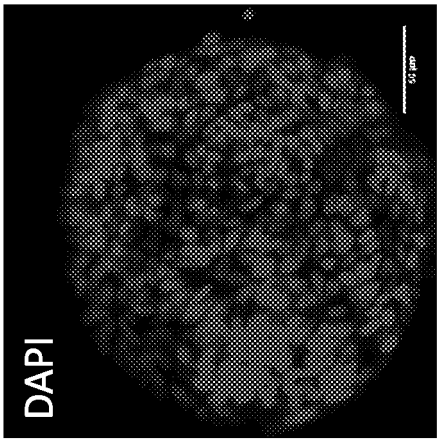
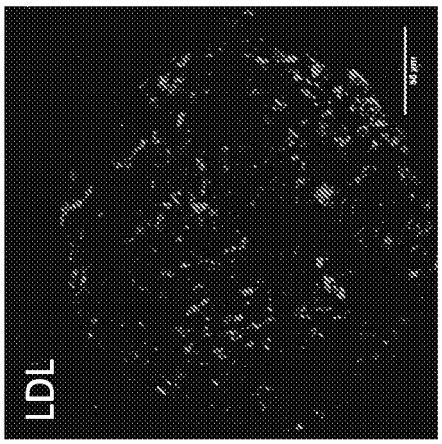


Fig. 27B





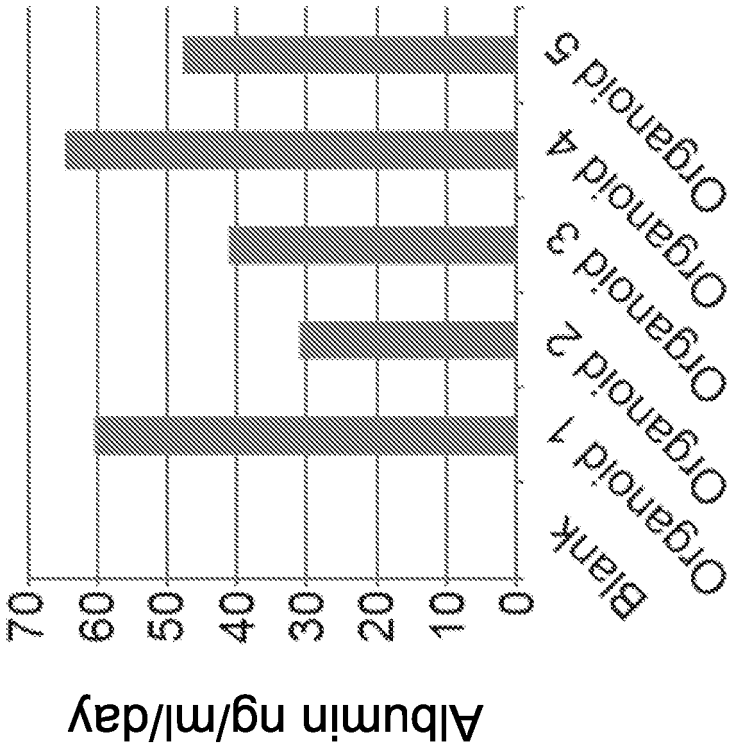


Fig. 28. Albumin secretion by hepatic organoid.

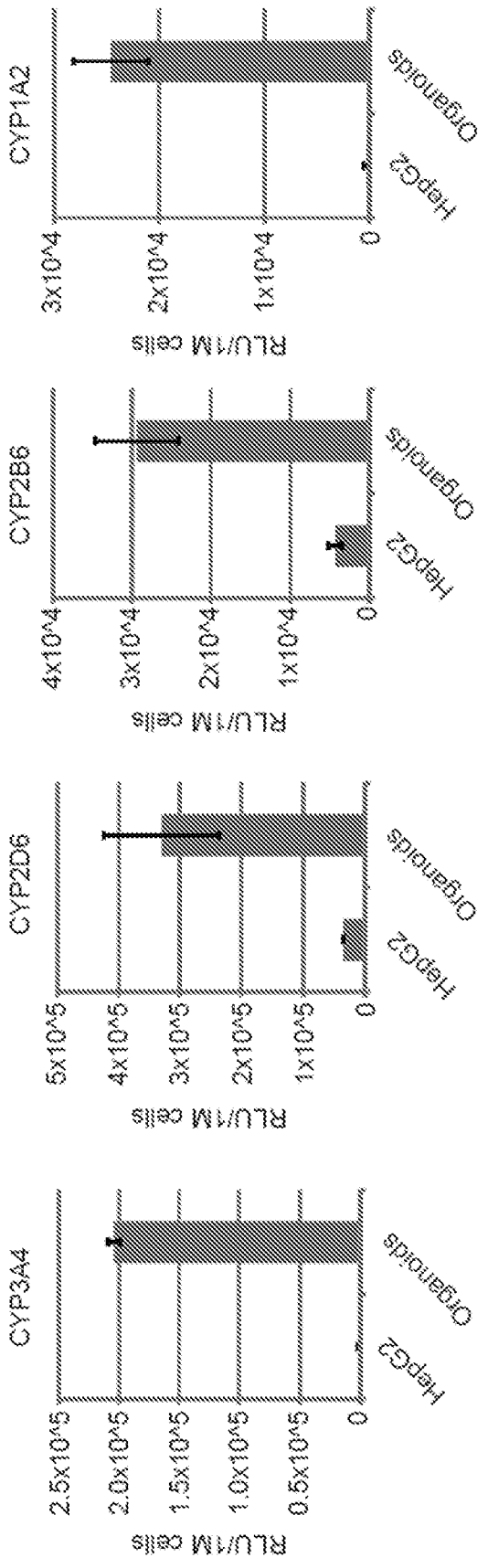


Fig. 29. Liver specific metabolic activities of the hepatic organoid.

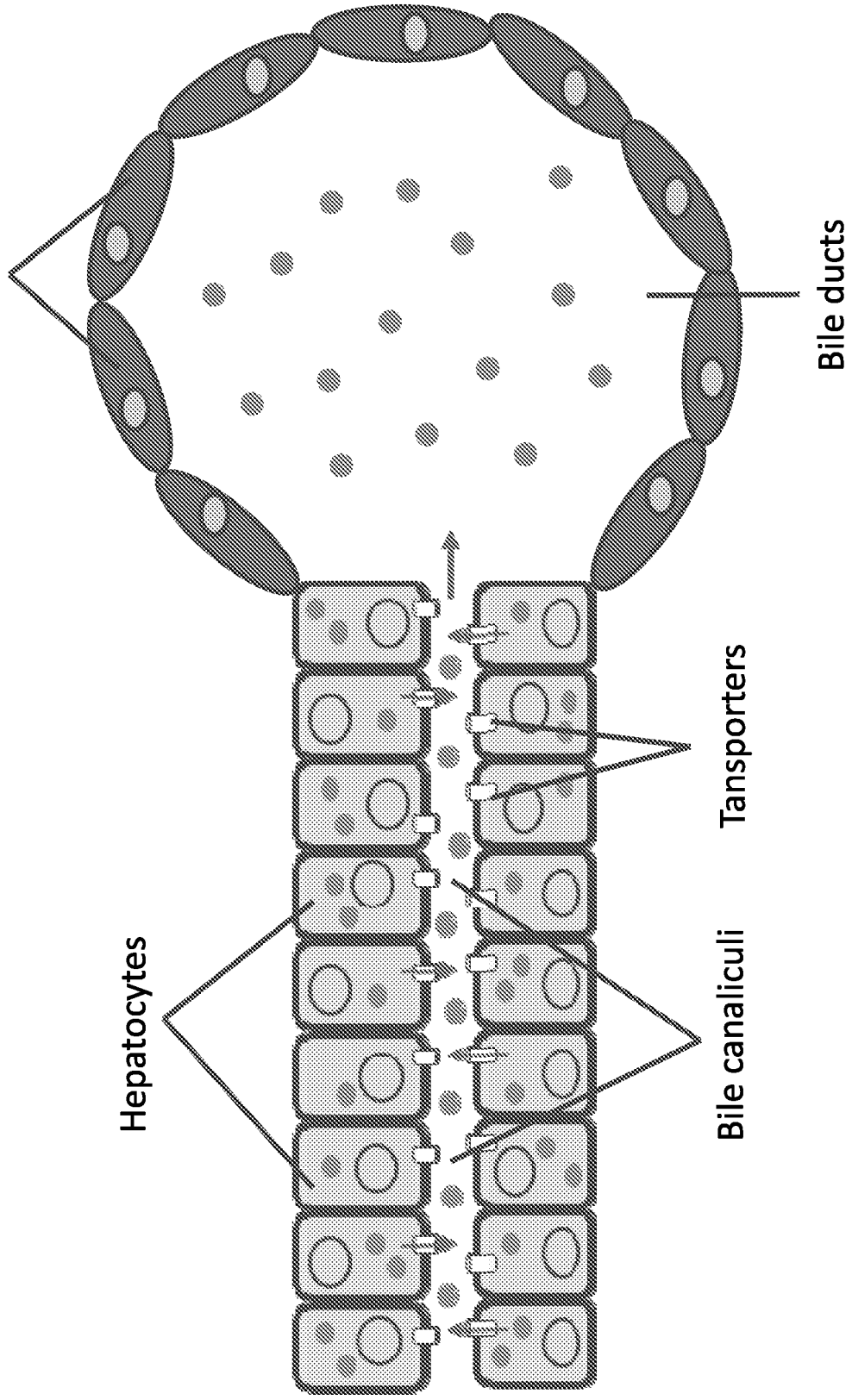
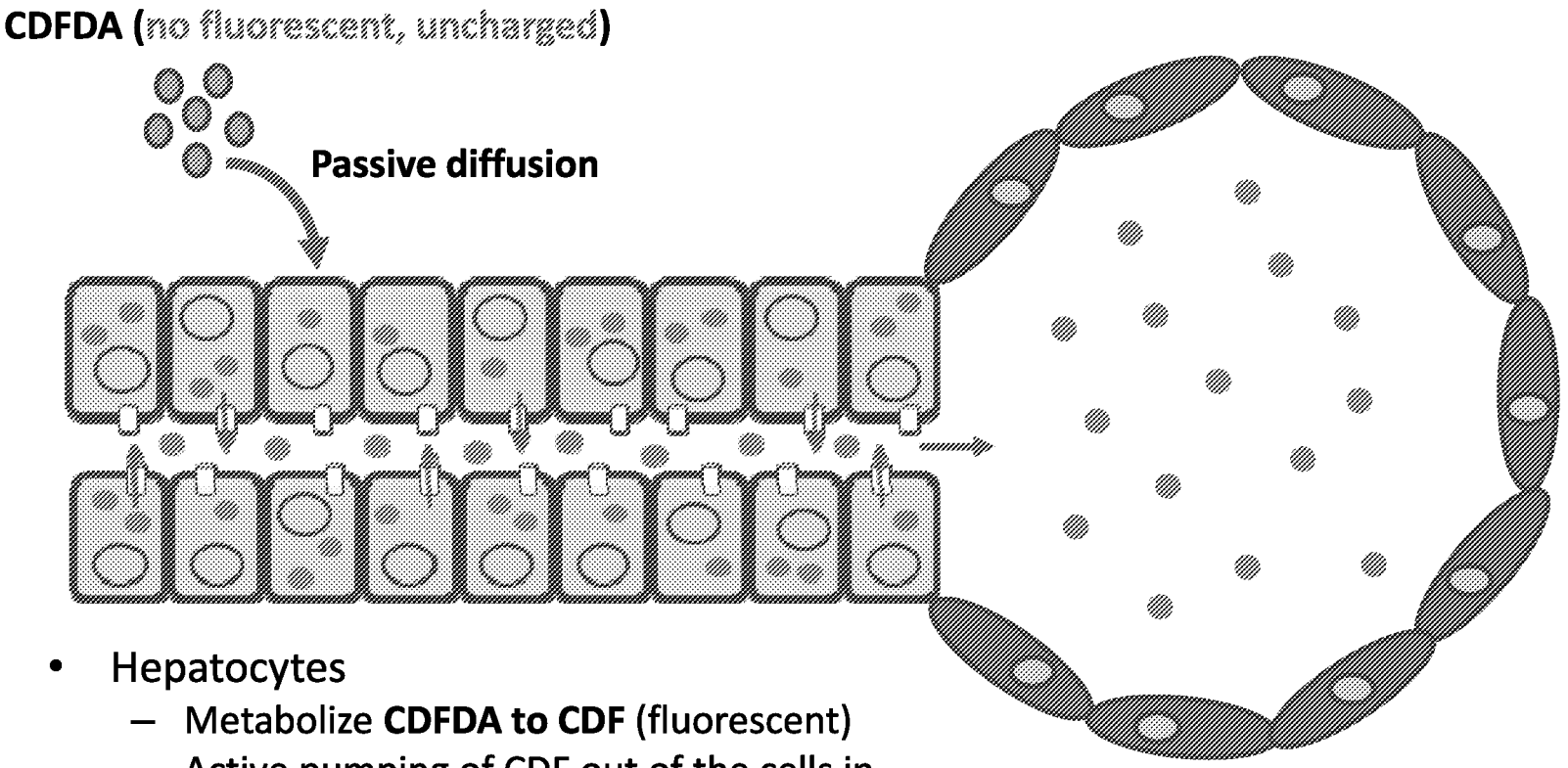


Fig. 30. Functional bile secretion system formed by hepatocytes and cholangiocytes in the liver.

Fig. 31. Imaging functional bile secretion system using CDFDA



- Hepatocytes
  - Metabolize **CDFDA to CDF** (fluorescent)
  - Active pumping of CDF out of the cells in the bile canaliculi
  - Transport of CDF into the bile duct like structures formed by the cyst

CDFDA conversion to CDF by hepatocytes in the organoids.

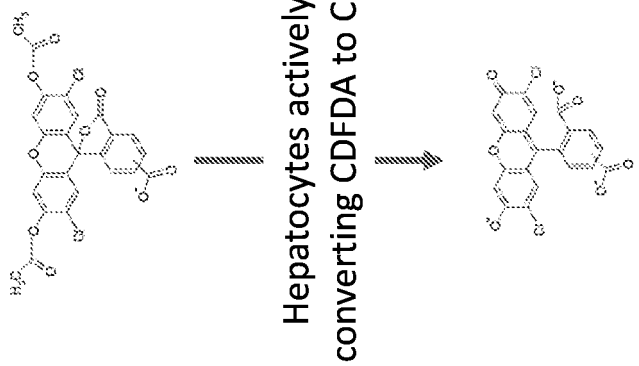


Fig. 32A

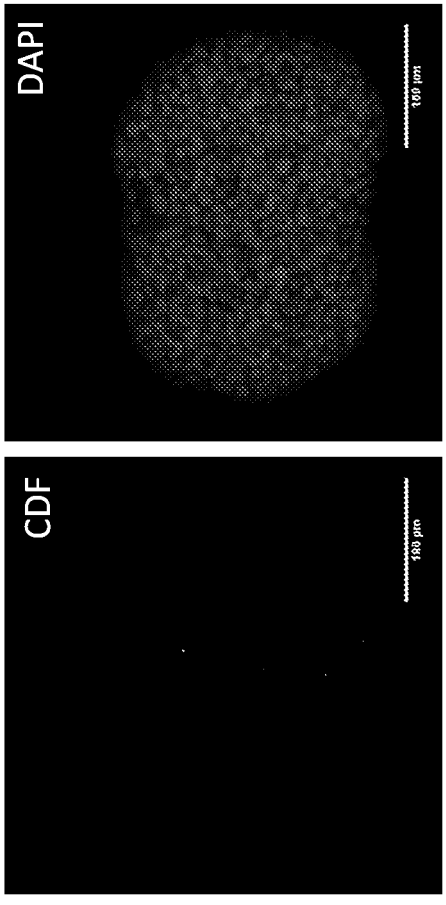
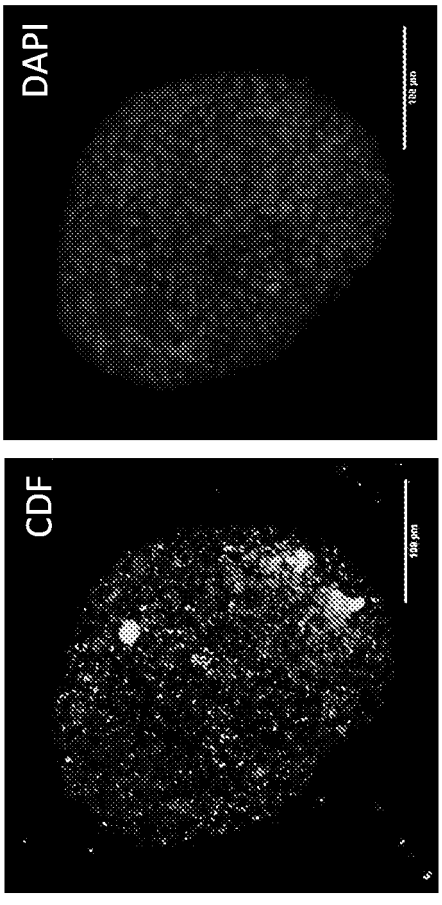


Fig. 32B



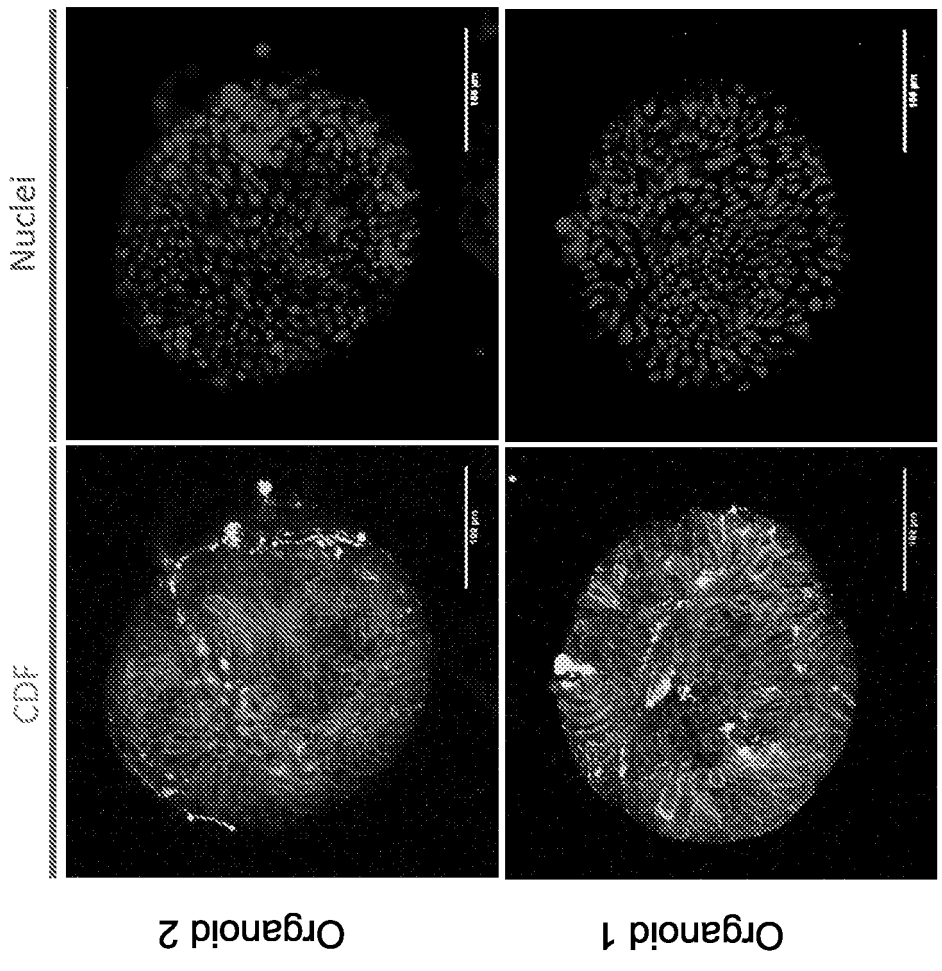


Fig. 33. Exporting CDF into the bile canaliculi network in the organoids.

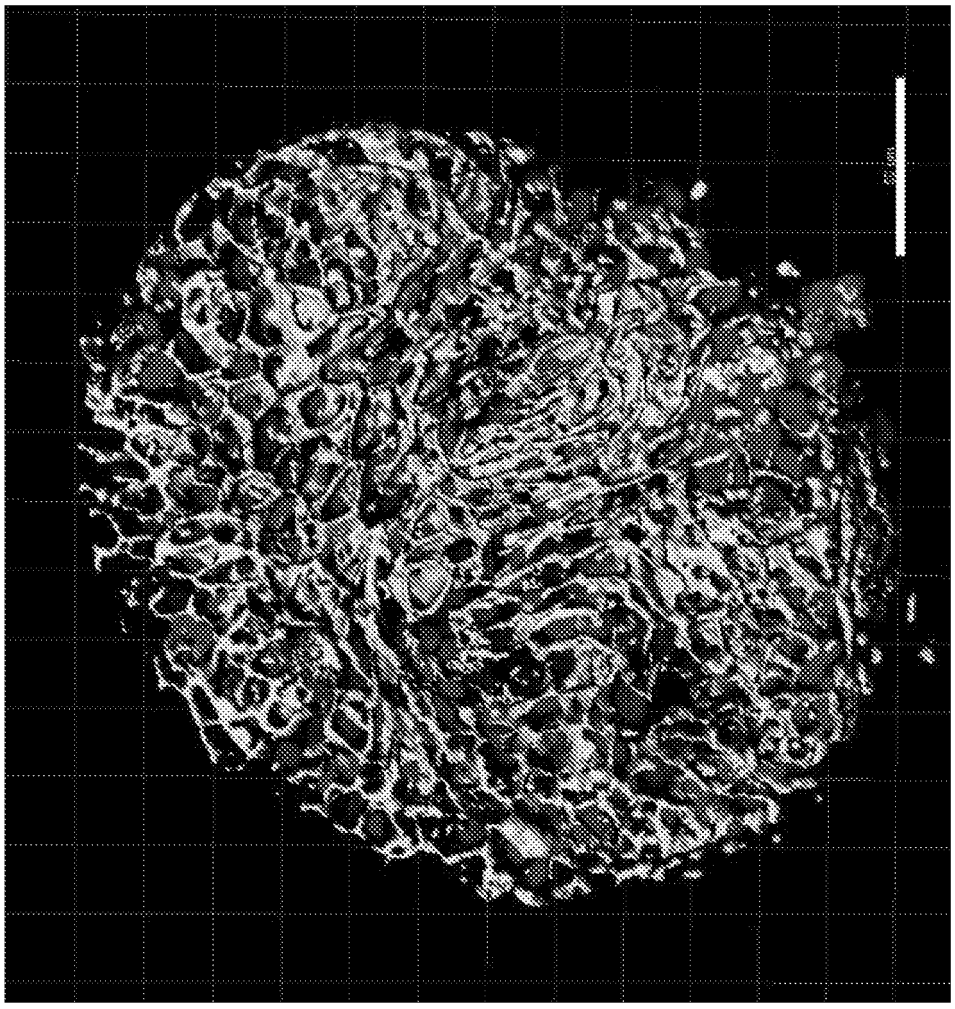


Fig. 34. 3D reconstructed image of bile canaliculi network within the organoid

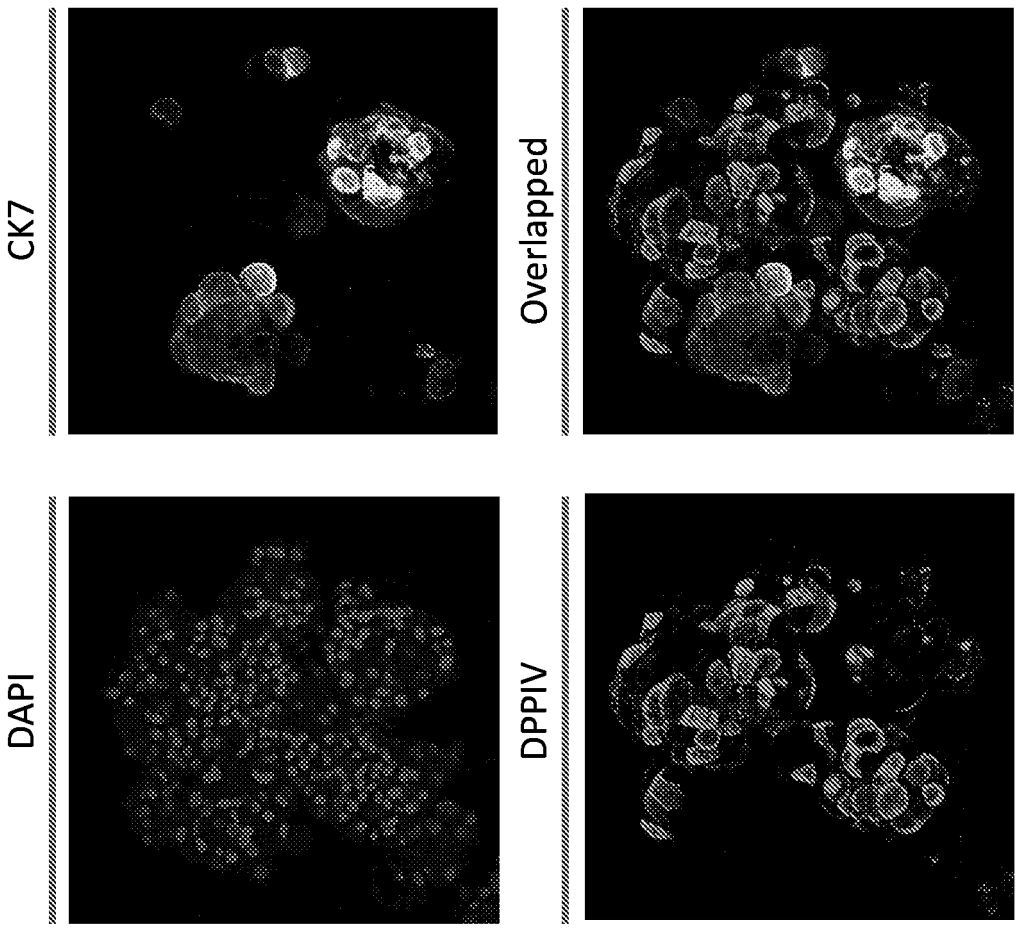


Fig. 35. Expression of bile canaliculi marker dipeptidyl peptidase IV (DPPIV) in the organoids

CDF transportation from the hepatocytes to the bile duct like structures formed by the cholangiocytes in the organoids

Fig. 36A

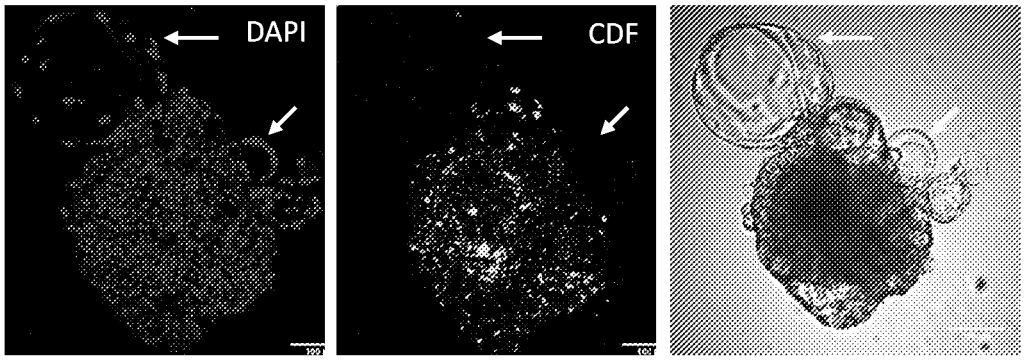


Fig. 36B

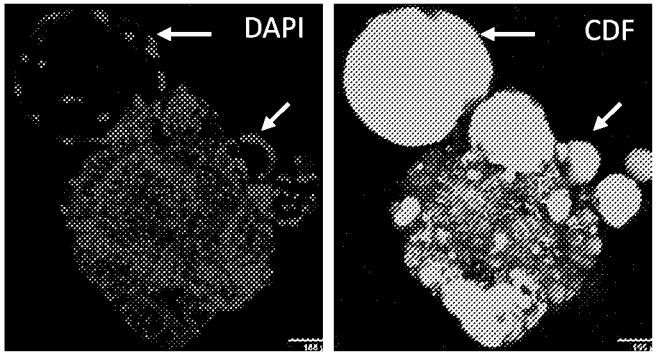


Fig. 36C

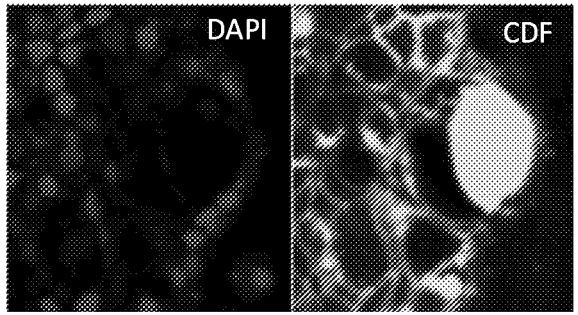
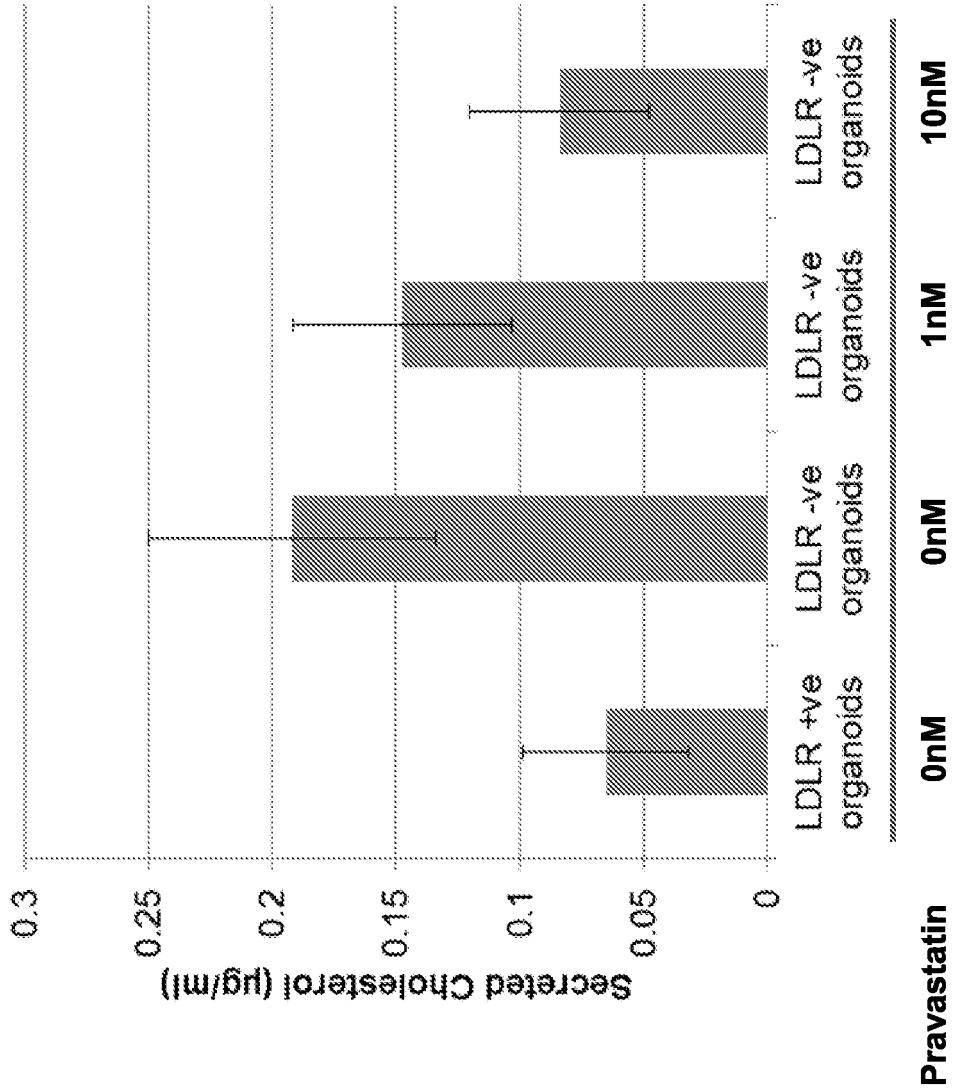


Fig. 37. LDLR KO organoids respond to cholesterol drugs.



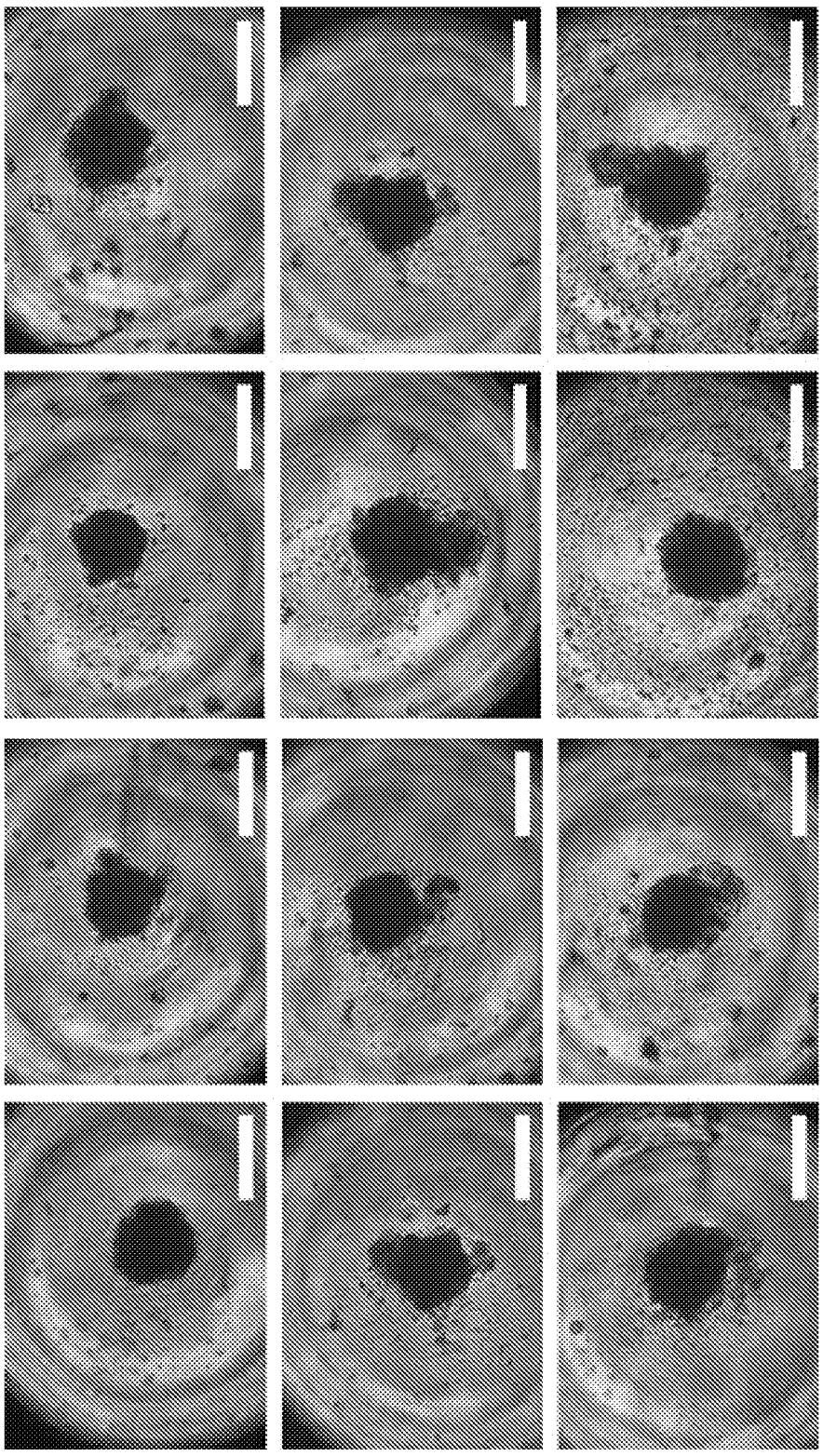


Fig. 38. High throughput generation of liver organoids

Individual organoids in high throughput system have comparable metabolic activity

Fig. 39A

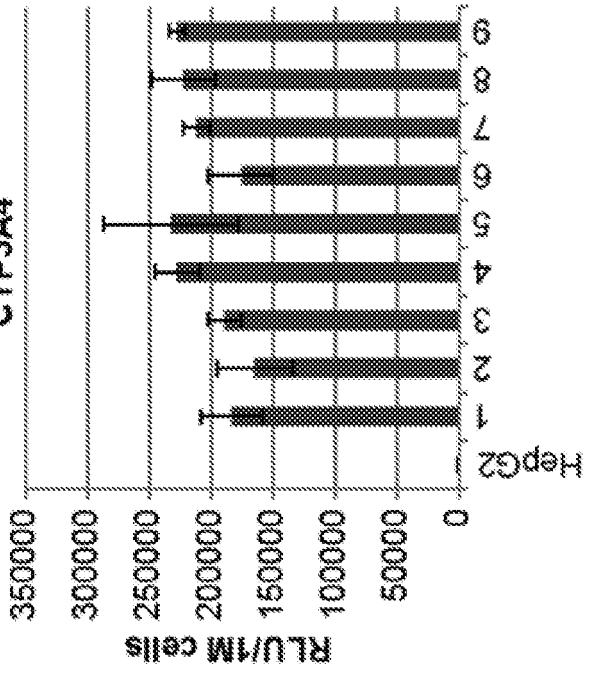


Fig. 39B

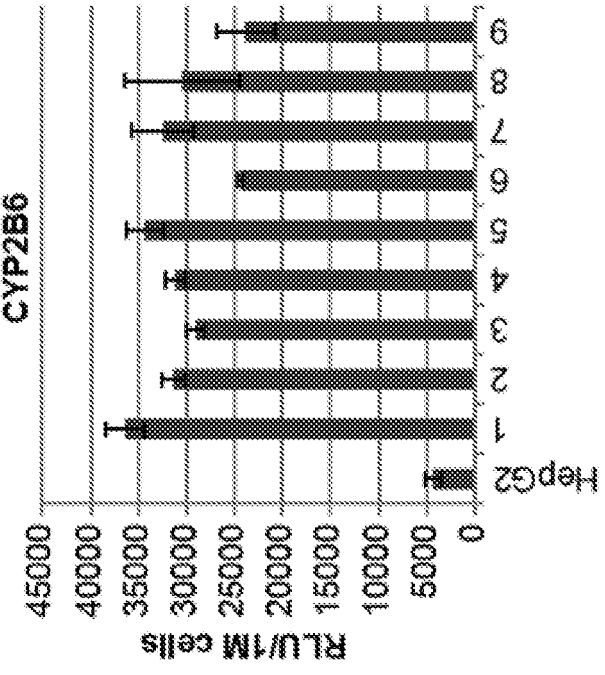
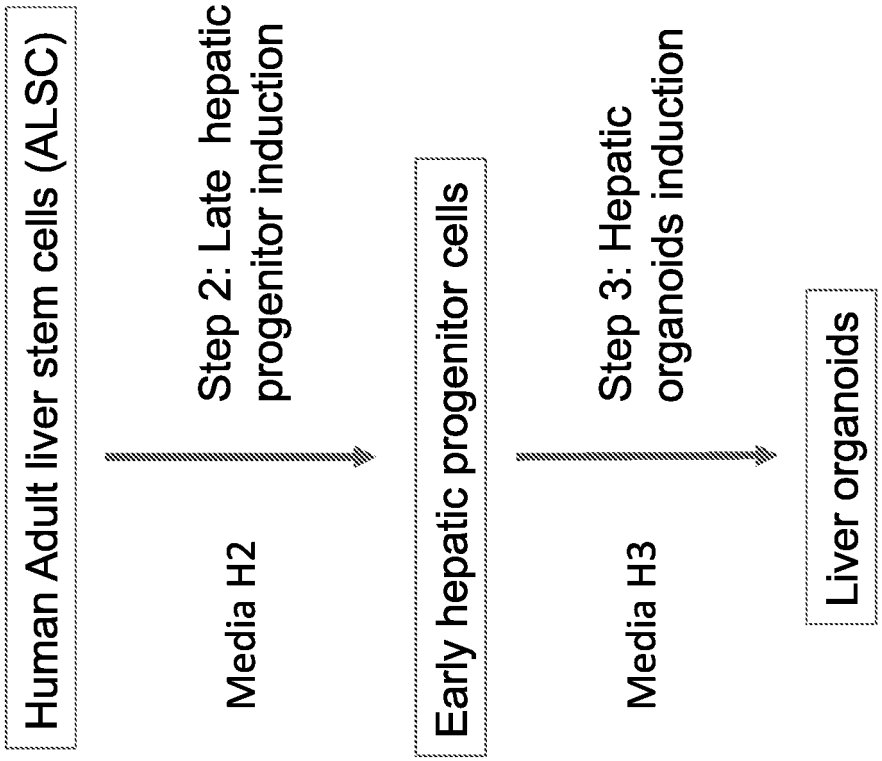


Fig. 40. Schematic of Liver organoid differentiation from adult liver stem cells (ALSC).



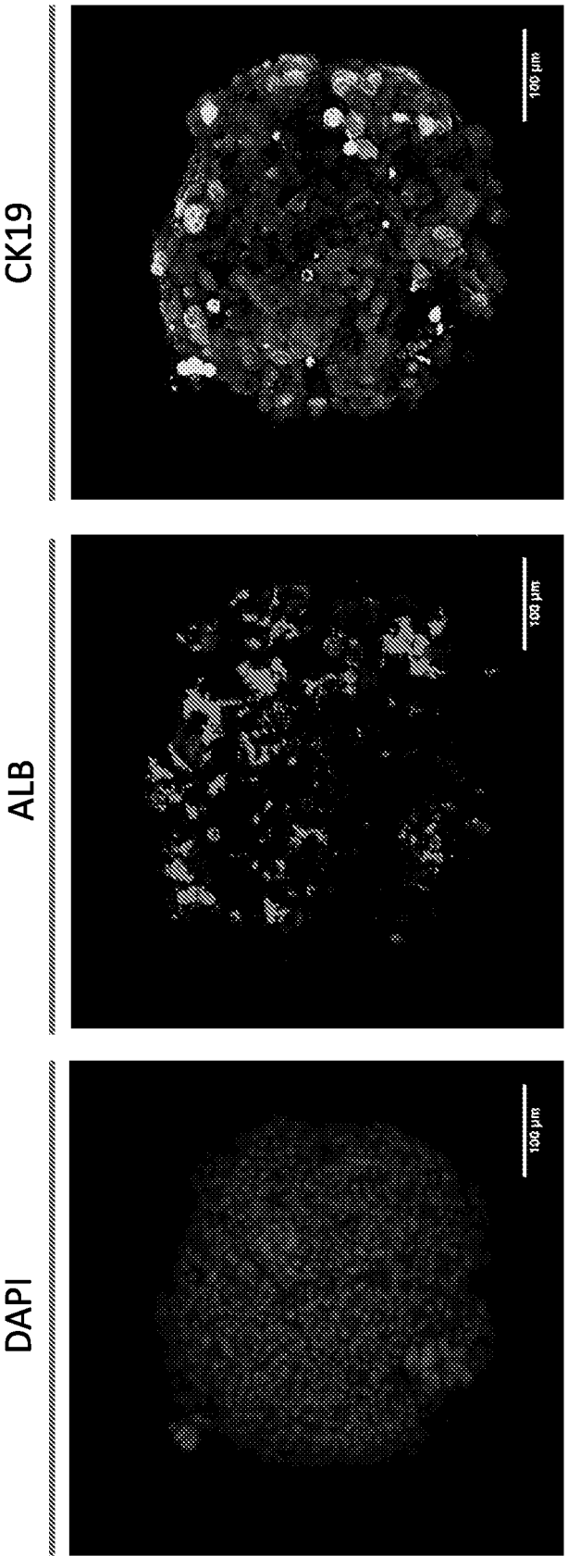


Fig. 41. Late hepatic progenitor formation from Adult liver stem cells (ALSC).

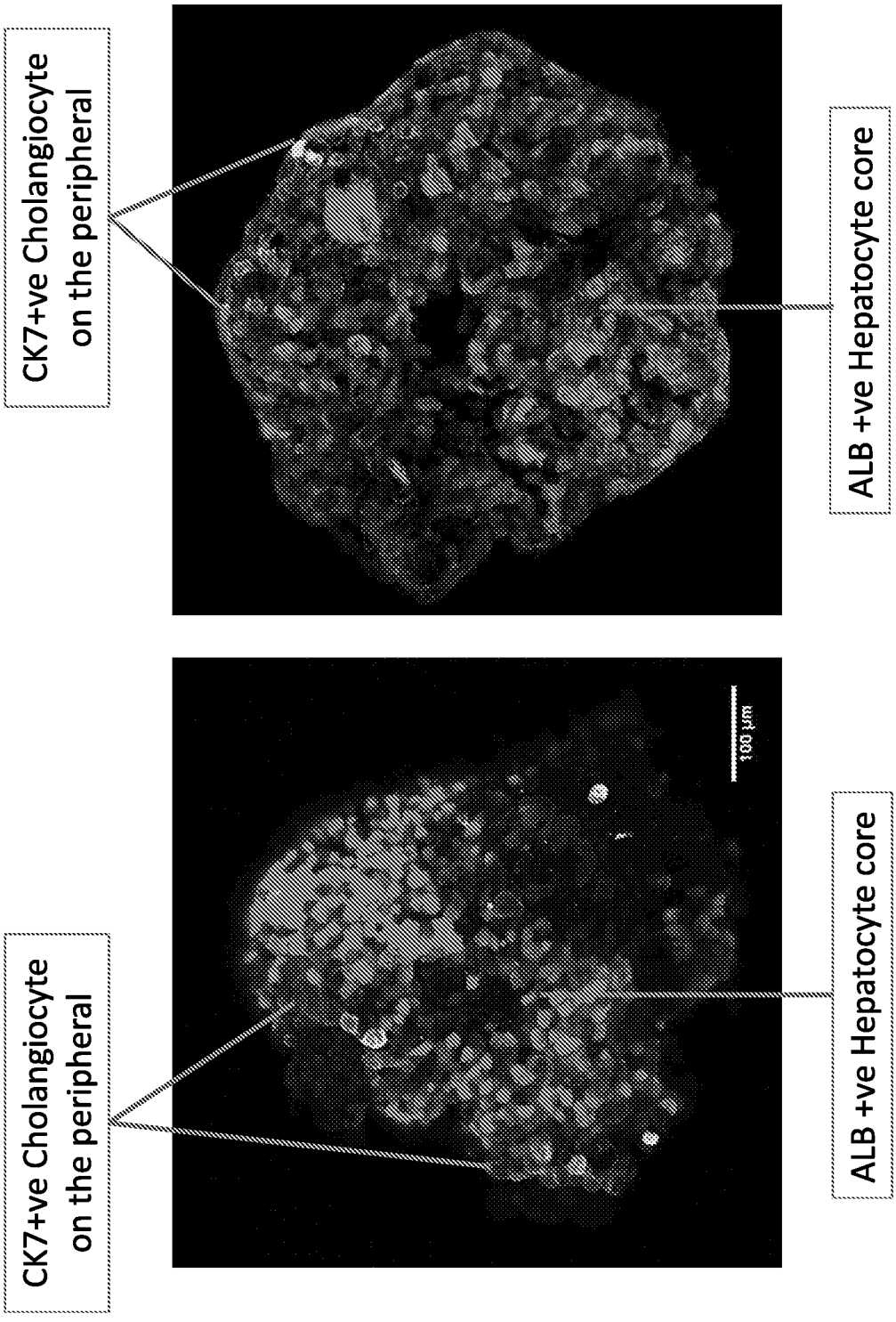


Fig. 42. Liver organoid generated using adult liver stem cells.

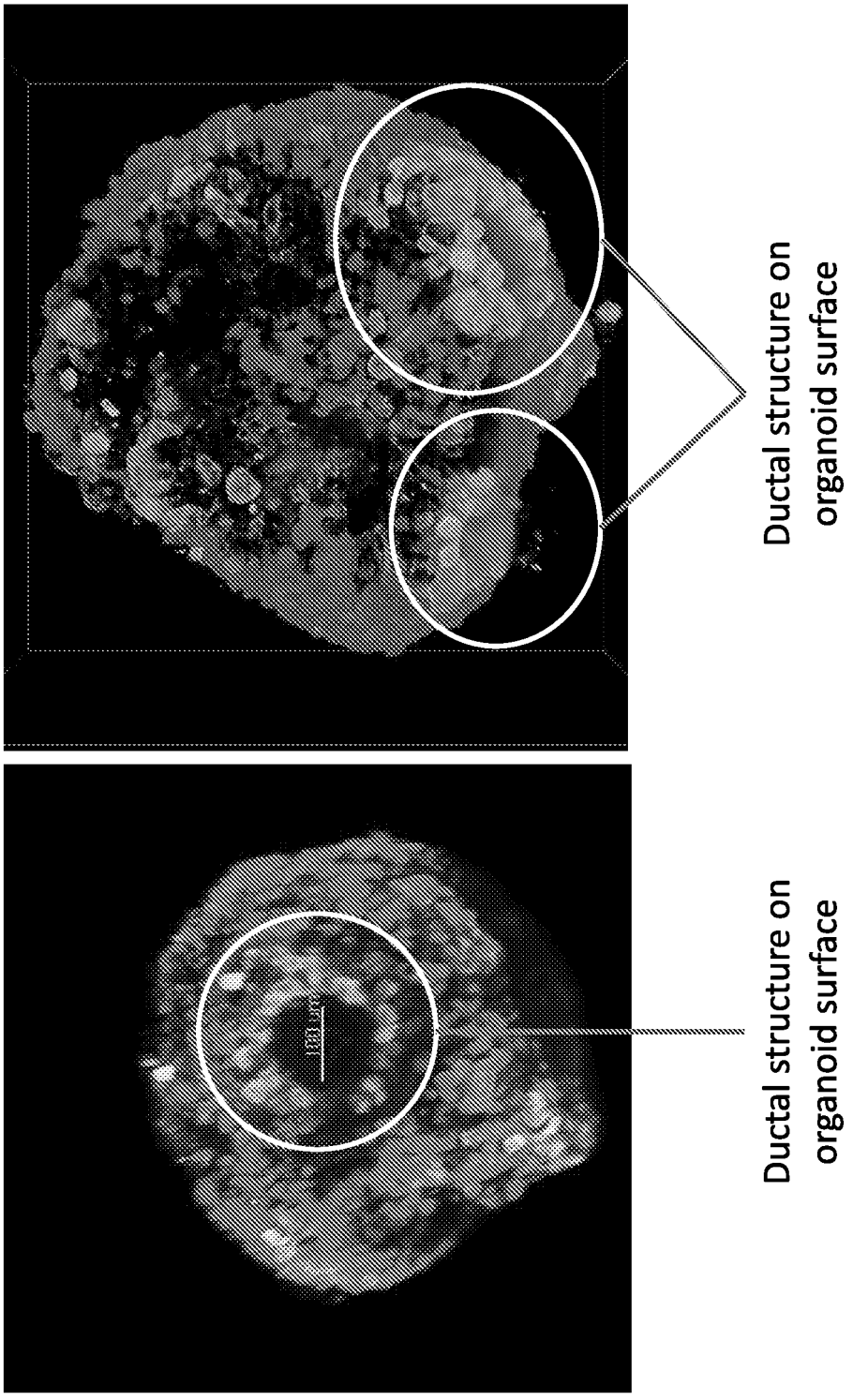


Fig. 43. 3D imaging of ALSC liver organoid with ductal structure

Fig. 44. Adult liver organoid expresses liver specific markers

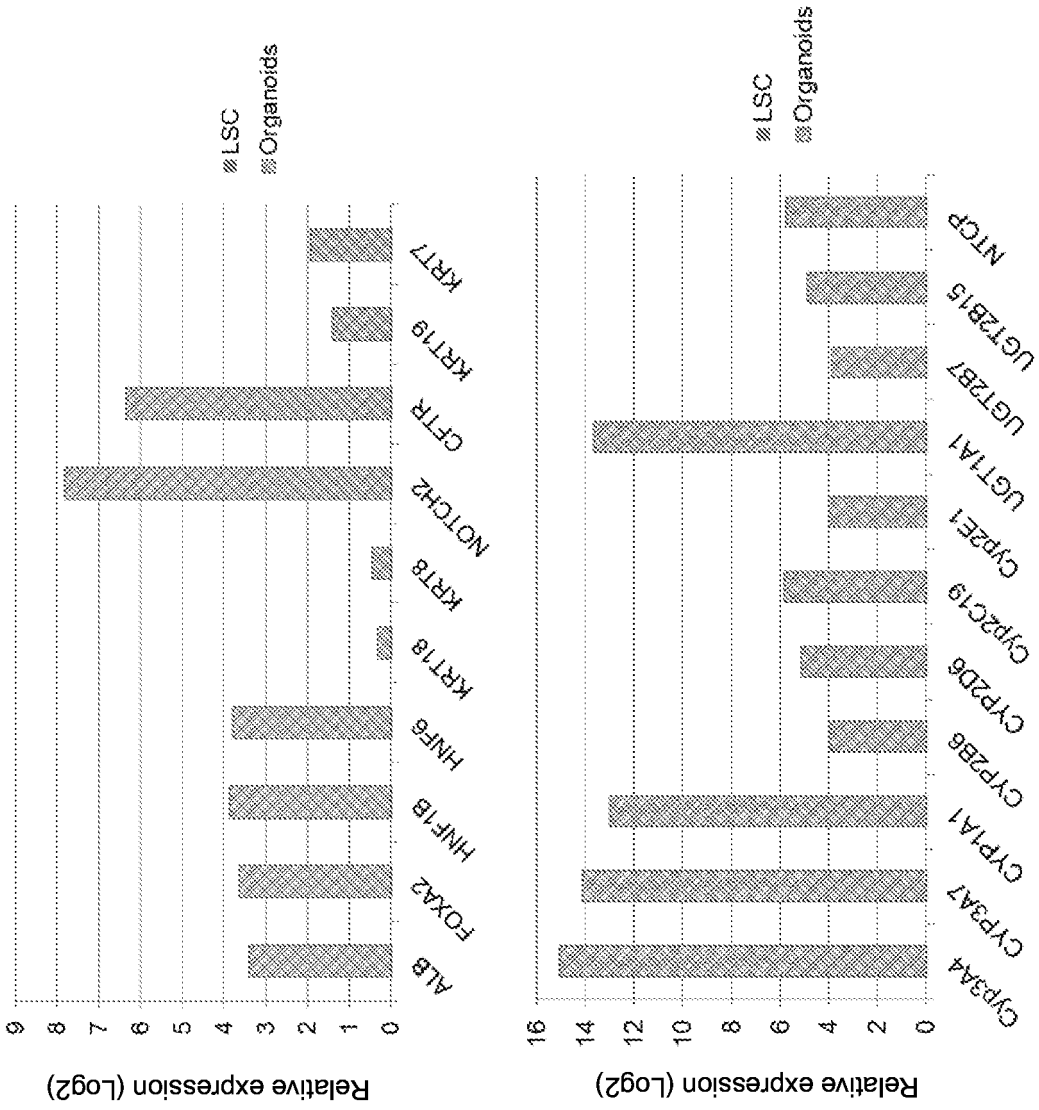
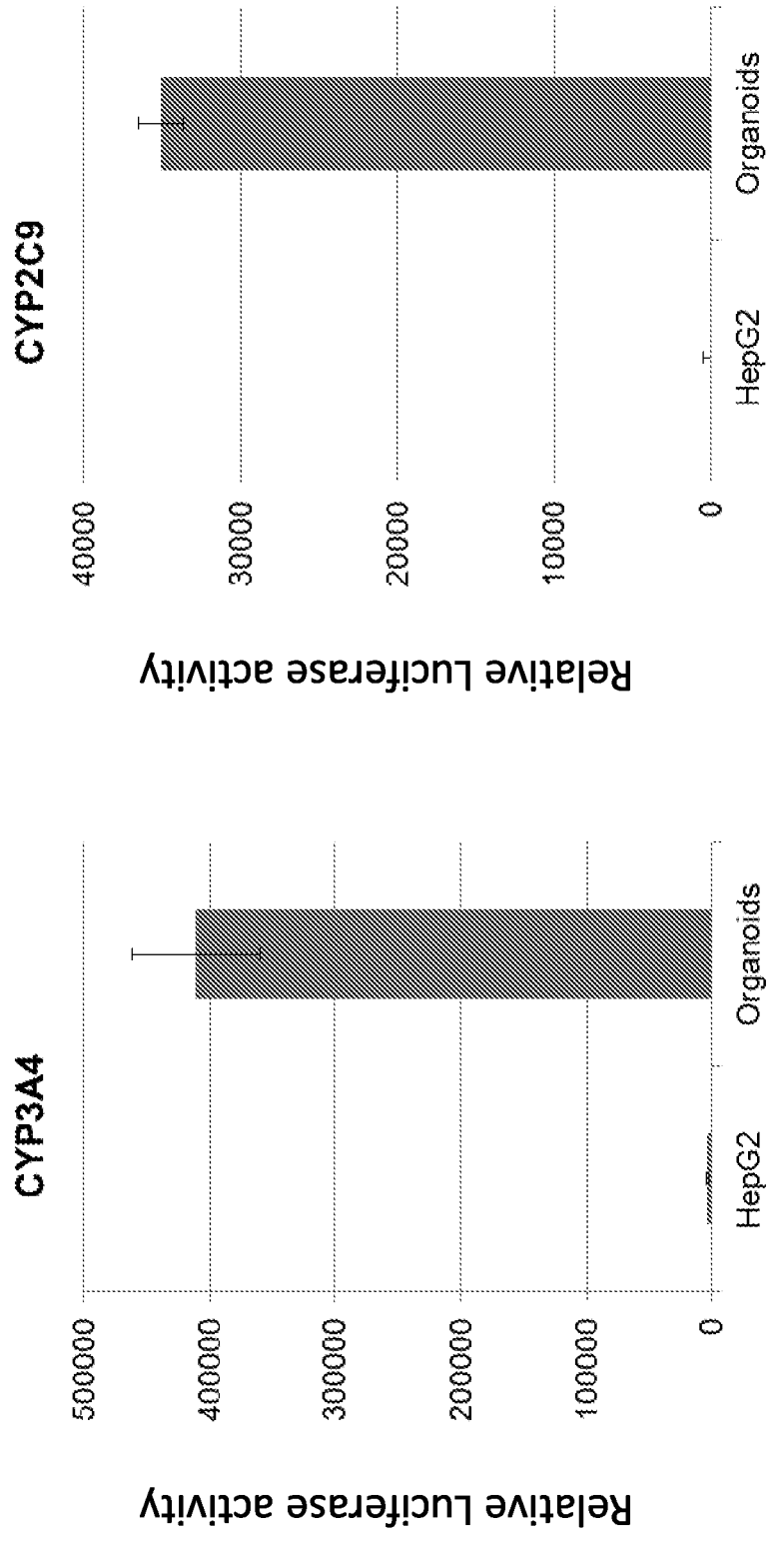


Fig. 45. Adult organoid exhibit liver specific metabolic activities



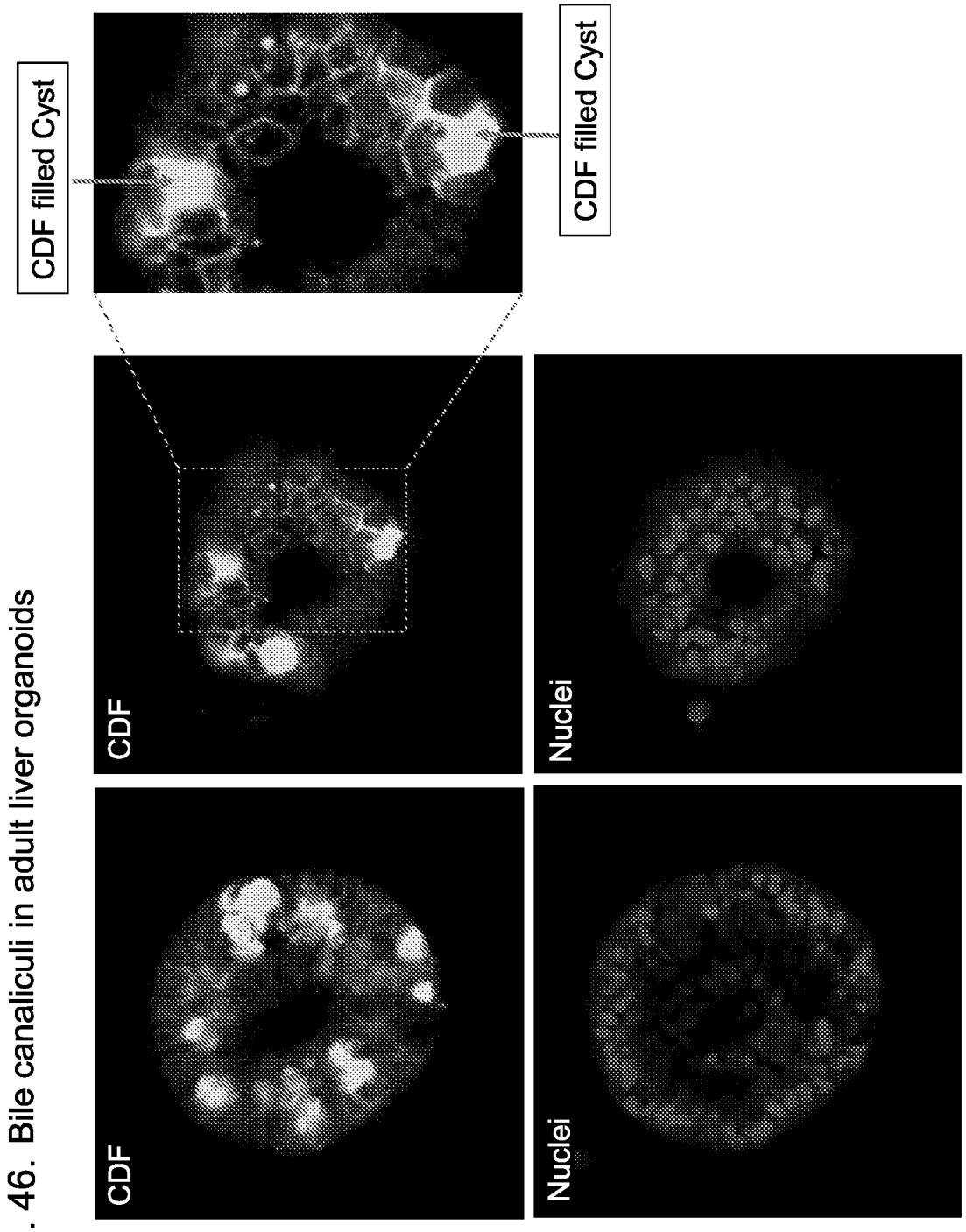


Fig. 46. Bile canaliculi in adult liver organoids

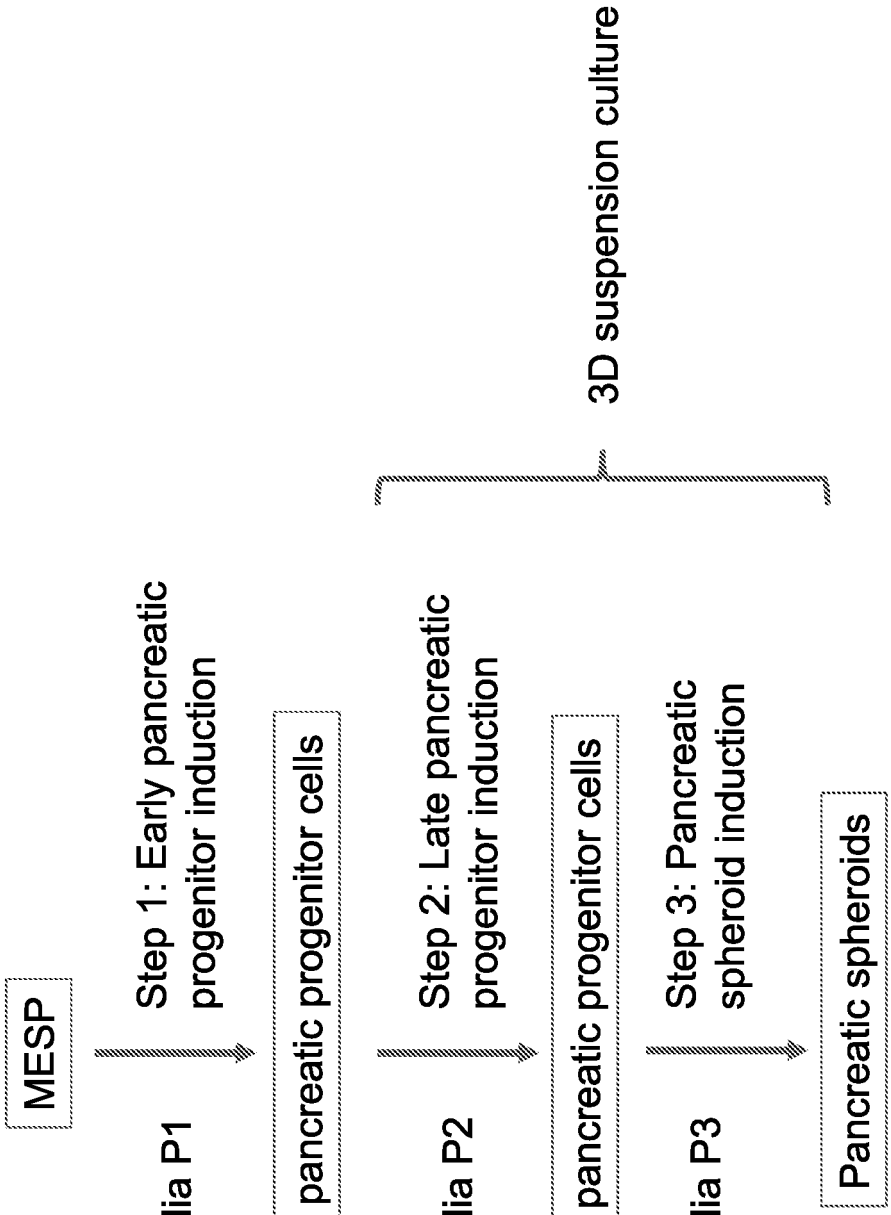


Fig. 47. Schematic of pancreatic spheroid production from MESP

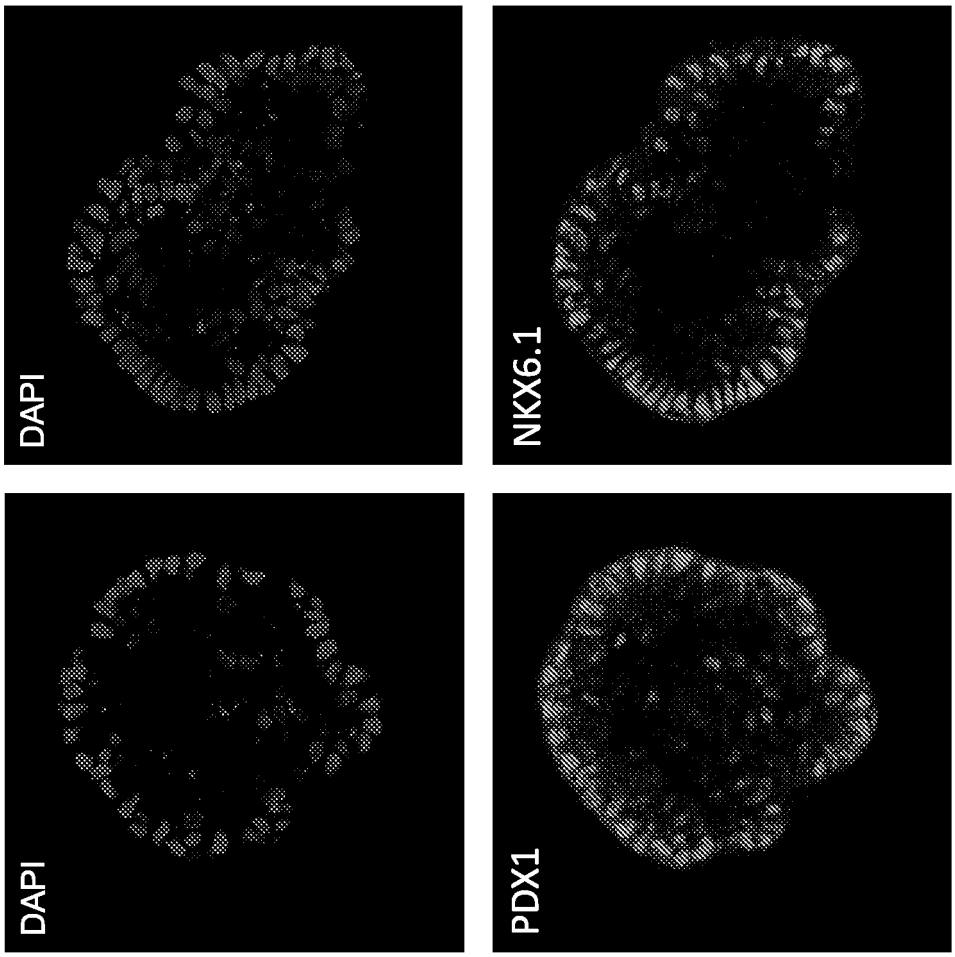


Fig. 48. Pancreatic spheroid generated from MESP

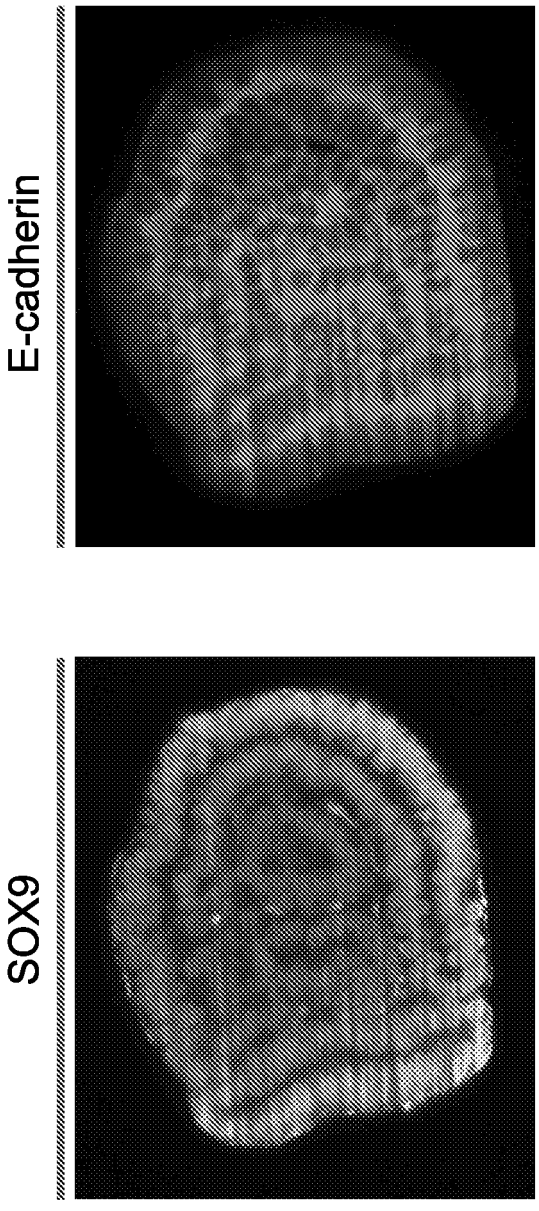


Fig. 49. Polarized E-cadherin expression in MESP